AMERICAN SOCIETY FOR MICROBIOLOGY | Infection and Immunity®

HOST RESPONSE AND INFLAMMATION

Whipworm Infection Promotes Bacterial Invasion, Intestinal Microbiota Imbalance, and Cellular Immunomodulation

Julieta Schachter,[b,c] Dayane Alvarinho de Oliveira,[a] Camila Marques da Silva,[b] Alba Cristina Miranda de Barros Alencar,[e] Michelle Duarte,[b] Matheus Müller Pereira da Silva,[b] Ana Claudia de Paula Rosa Ignácio,[d] Eduardo José Lopes-Torres[a]

[a]Laboratório de Helmintologia Romero Lascasas Porto, Departamento de Microbiologia, Imunologia e Parasitologia, Faculdade de Ciências Médicas, Universidade do Estado do Rio de Janeiro, Rio de Janeiro, RJ, Brazil

[b]Instituto de Biofísica Carlos Chagas Filho, Universidade Federal do Rio de Janeiro, Cidade Universitária, Rio de Janeiro, RJ, Brazil

[c]Universidad de Buenos Aires, Consejo Nacional de Investigaciones Científicas y Técnicas, Instituto de Química y Fisico-Química Biológicas (IQUIFIB) Prof. Alejandro C. Paladini, Facultad de Farmacia y Bioquímica, Junín, Buenos Aires, Argentina

[d]Departamento de Microbiologia, Imunologia e Parasitologia, Faculdade de Ciências Médicas, Universidade do Estado do Rio de Janeiro, Rio de Janeiro, RJ, Brazil

[e]Parasitologia Clínica, Departamento de Patologia, Faculdade de Medicina da Universidade Federal Fluminense, Hospital Universitário Antonio Pedro, Niterói, Brazil

Julieta Schachter and Dayane Alvarinho de Oliveira contributed equally to this article. Author order was decided based on the involvement of Julieta Schachter in the work conceptualization.

ABSTRACT Infections with *Trichuris trichiura* are among the most common causes of intestinal parasitism in children worldwide, and the diagnosis is based on microscopic egg identification in the chronic phase of the infection. During parasitism, the adult worm of the trichurid nematode maintains its anterior region inserted in the intestinal mucosa, which causes serious damage and which may open access for gut microorganisms through the intestinal tissue. The immune-regulatory processes taking place during the evolution of the chronic infection are still not completely understood. By use of the Swiss Webster outbred mouse model, mice were infected with 200 eggs, and tolerance to the establishment of a chronic *Trichuris muris* infection was induced by the administration of a short pulse of dexamethasone during nematode early larval development. The infected mice presented weight loss, anemia, an imbalance of the microbiota, and intense immunological cell infiltration in the large intestine. It was found that mice have a mixed Th1/Th2/Th17 response, with differences being found among the different anatomical locations. After 45 days of infection, the parasitism induced changes in the microbiota composition and bacterial invasion of the large intestine epithelium. In addition, we describe that the excretory-secretory products from the nematode have anti-inflammatory effects on mouse macrophages cultured *in vitro*, suggesting that *T. muris* may modulate the immune response at the site of insertion of the worm inside mouse tissue. The data presented in this study suggest that the host immune state at 45 days postinfection with *T. muris* during the chronic phase of infection is the result of factors derived from the worm as well as alterations to the microbiota and bacterial invasion. Taken together, these results provide new information about the parasite-host-microbiota relationship and open new treatment possibilities.

KEYWORDS helminth, nematodes, *Trichuris muris*, immune response, excretory-secretory products, intestine, *Trichuris*, excretory-secretory, infectious disease, intestine, microbiota, neglected disease

Infections with soil-transmitted helminths affect more than a quarter of the world's population, causing morbidity and disability, especially in people living in regions with poor access to water and public health (1). According to a 2013 estimate, whipworms of the species *Trichuris trichiura* infect 477 million individuals worldwide,

Citation Schachter J, Alvarinho de Oliveira D, da Silva CM, de Barros Alencar ACM, Duarte M, da Silva MMP, Ignácio ACDPR, Lopes-Torres EJ. 2020. Whipworm infection promotes bacterial invasion, intestinal microbiota imbalance, and cellular immunomodulation. Infect Immun 88:e00642-19. https://doi.org/10.1128/IAI.00642-19.

Editor De'Broski R. Herbert, University of Pennsylvania

Address correspondence to Eduardo José Lopes-Torres, eduardo.torres@uerj.br.

Received 15 August 2019
Returned for modification 9 September 2019
Accepted 6 December 2019
Accepted manuscript posted online 16 December 2019
Published 20 February 2020

with the highest prevalence being in children (2). Trichuriasis, as well as other helminthiases, is present at a high incidence, especially in people with nutritional deficiency (3, 4). Other species of the genus *Trichuris* with a global distribution are parasites of other mammals, including animals of economic and veterinary interest (5). All trichurid nematodes present a unique strategy for their parasitism, forming an intratissue niche inside the cells of the mammalian large intestine, causing alterations and disruption of the tissue cover (6). In humans, the colitis induced by *Trichuris* is being studied as a possible major environmental driver of inflammatory bowel disease (7). The specific host-parasite relationship developed for trichurid nematodes was studied before (8–11), but the immune-regulatory processes involved in maintenance of the chronic infection remain unknown.

Trichuris muris has been widely used in experimental mouse models to study host-parasite interactions. In both mice and humans, *Trichuris* eggs hatch in the small intestine, and the larvae then migrate to the large intestine, invading the intestinal mucosa (8). The nematode grows and moves inside the epithelial layer, with the anterior end remaining inserted in the host tissue and the posterior region remaining free in the lumen, causing damage to the intestinal epithelium (12). Once they are fixed, *Trichuris* worms cause inflammation at the site of intracellular attachment and induce a colitis-like pathology (13).

A distinctive morphological characteristic of the *Trichuris* genus is the presence of a bacillary band in the anterior region of the body, which is formed by bacillary glands, stichocytes, and cuticular inflations and which is hypothesized to play a role in parasite invasion and maintenance in the host tissue (14, 15). The parasite's anterior end excretes and secretes products (excretory-secretory [ES] products) that can be collected from the media of *in vitro* cultures and that have been described to be factors governing host-parasite interactions (16). Considering the particular niche of *Trichuris*, which grows inside the intestinal epithelium, it seems reasonable to expect that the ES products from this nematode may have an important role in parasitism. Previous works identified several proteins and microRNAs secreted by *T. muris* (17), and proteins isolated from ES products were also tested as a vaccine, with promising results (18); however, the effects on the immune response have not been fully elucidated.

It was shown that *T. muris* infection affects the composition of the gut microbiota, decreasing the diversity of bacterial communities and changing the abundance of some particular genera (19, 20). On the other hand, contact between commensal bacteria and *T. muris* eggs is required for hatching of the eggs (21). During a *Trichuris* infection, depletion of the microbiota with antibiotic treatment leads to the establishment of a chronic infection, indicating that intestinal bacteria are associated with the worm establishment inside the intestine (21, 22). However, the influence of the intestinal microbiota in the regulation of the host immune response and in the pathophysiological evolution of the infection remains to be established.

The pathophysiology of trichuriasis is complex, and its development depends on host genetic characteristics, nematode mechanical and biochemical actions, ES product activity, and changes to the microbiota, with all these different factors having effects on the host immune response. Two major immune responses were characterized in laboratory mice, and these depended on the inbred mouse strain: a Th2-type immune response, which leads to parasite expulsion, and a Th1-type response, which is associated with the establishment of a chronic infection (8). Although the Th2-type response is associated with host protection and Th1 responses are associated with susceptibility to infection, the immunological balance in a chronic *Trichuris* infection was only barely explored (18, 23). An outbred mouse strain was used as an experimental model in this study, and tolerance to the establishment of a chronic infection was induced by the administration of a short pulse of dexamethasone during early larval development of the nematode in an attempt to mimic the conditions of populations in which the individuals have a nonuniform genetic background and an immune profile state that allows infection.

The present study characterizes the alterations promoted by *T. muris* in the epithelial

layers of the large intestine as well as the local and systemic immune responses at a specific time point in the initial chronic phase of infection, which was at 45 days postinfection. It was found that mice have a mixed Th1/Th2/Th17 response, with differences being seen among the different anatomical locations. It was shown that chronic infection induces changes in the microbiota composition and bacterial invasion of the large intestine submucosa. This study also found that ES products have anti-inflammatory effects on mouse macrophages, suggesting that *T. muris* may modulate the immune response at the site of insertion in mouse tissue. It is proposed here that the host's immune status observed during chronic *T. muris* infection is the result of factors from the nematode as well as changes in the microbiota composition and bacterial invasion. These novel data can contribute to the development of new guidelines for treatments with anthelmintics and antibiotics as well as the administration of prebiotics and/or probiotics for modulation of the microbiota.

RESULTS

Chronic *T. muris* infection causes a reduction in body weight and alterations in abdominal organs. Initially, the impact of chronic *T. muris* infection was observed in mice when the animals' health status was evaluated after 45 days of infection. The infected mice started to eliminate eggs on the 35th day after infection, and at that time, remarkable hair loss was observed in the infected animals. The infection reduced the mouse body weight, with the average weight being 36.53 $\pm$ 3.22 g for the control mice and 33.17 $\pm$ 5.29 g for the infected mice. During necropsy, it was possible to identify macroscopic alterations in the abdominal cavity, such as greater viscera adhesion and cecal hypertrophy and rigidity. An average of 82.5 $\pm$ 7.14 nematodes was recovered from each infected animal.

***T. muris* infection promotes rupture and disorganization of the intestinal epithelium, accompanied by immune cell infiltration.** Histopathological analysis allowed identification of the normal aspect of the three layers of the large intestine in the control animals and structural alterations in the tissues of the chronically infected mice, with the anterior region of *T. muris* being found to be inserted in the mucosa of the host intestinal epithelium of the infected mice (Fig. 1A). In the control mice, the mucosa muscular layer was very thin and almost imperceptible. However, in the infected mice, it was possible to visualize that layer very clearly (Fig. 1A, right). Morphometric analyses showed a significant thickening of the mucosa (466 $\pm$ 143 μm), submucosa (327 $\pm$ 127 μm), and muscularis (169 $\pm$ 69 μm) layers in the infected mice compared with the thickness of the mucosa (239 $\pm$ 89 μm), submucosa (83 $\pm$ 19 μm), and muscularis (71 $\pm$ 23 μm) layers of the control animals (Fig. 1B).

Morphological characterization of the cells found in the intestinal epithelium showed that the thickness alteration observed in chronically infected mice was promoted by changes in the volume and number of each infected mouse's own tissue cells and by inflammatory cell infiltration. In the mucosal layer of the infected mice, an increase in the number and volume of goblet cells compared with the number and volume of goblet cells in the controls was observed (Fig. 1A, insets for control and infected mice, and Fig. 1C). The histopathological images enabled the identification of a polymorphonuclear cell infiltrate in the intestinal sections of the infected mice (Fig. 2A), contributing to the increase in the height of the mucosal and submucosal layers. Quantification of the stained cells in the submucosa showed that the amounts of neutrophils, eosinophils, macrophages, and lymphocytes were significantly higher in the infected mice than in the control animals (Fig. 2B).

Hematological and biochemical alterations promoted by chronic *T. muris* infection. Subsequently, the hematological parameters for control and infected mice were analyzed. The infected mouse group showed a significant increase in the leucocyte (white blood cell [WBC]) numbers, together with a decrease in the glucose concentrations in the blood, compared with the findings for the control group (Table 1). In *T. muris*-infected mice, significant decreases in the number of red blood cells (RBCs) and hematocrit (Hct) were also detected, and these decreases were accompa-

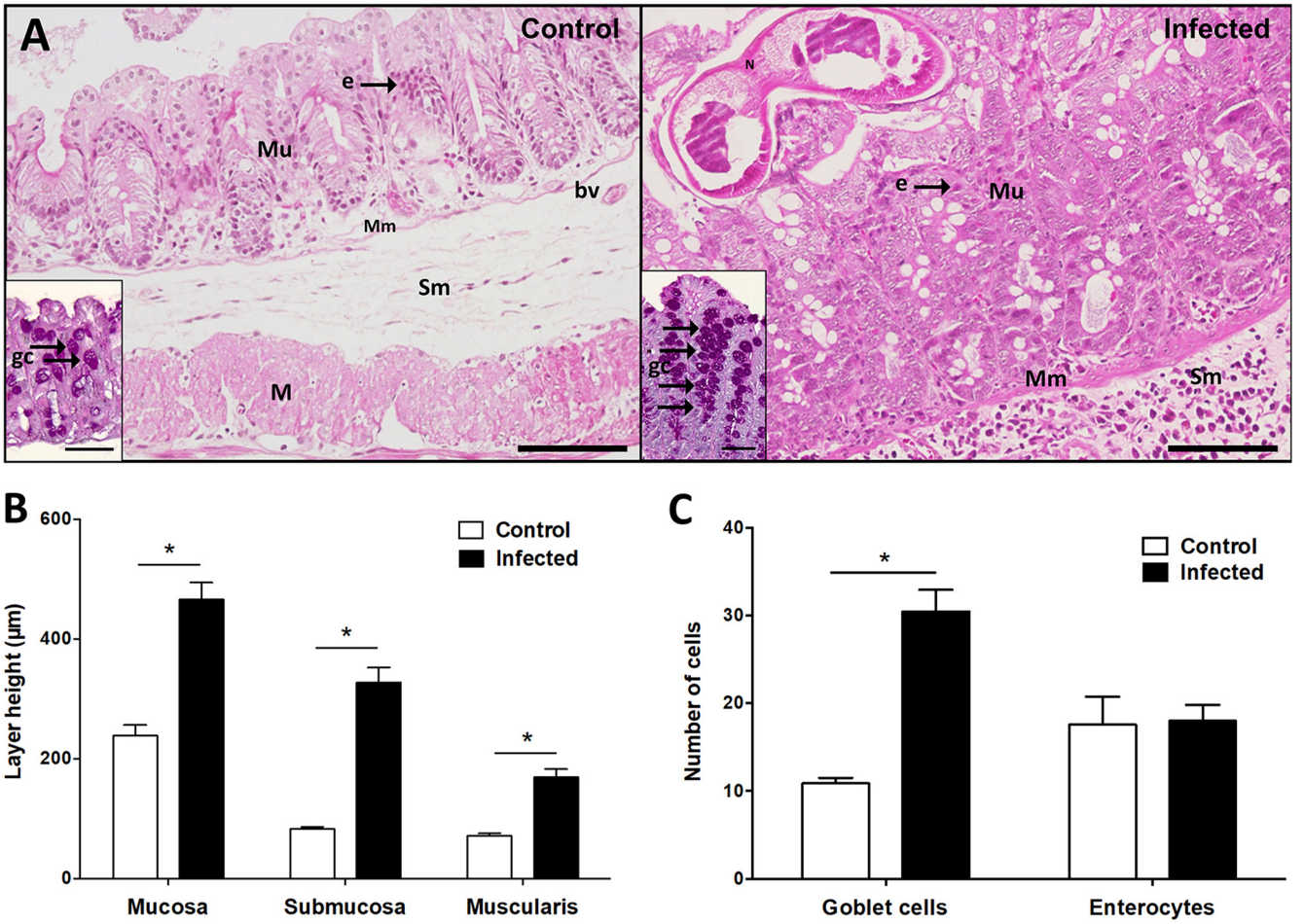

FIG 1 Histological section of large intestine (cecum) stained with hematoxylin and eosin, showing the morphology and morphometry of the large intestine layers. (A) (Left) Section from control animals showing the integrity of the mucosa, submucosa, and muscularis layers. (Right) Section from infected mice showing the nematode *T. muris* inserted in the mucosa and submucosa with infiltration. Bars, 100 μm. (Insets) PAS staining showing goblet cells in control and infected mucosal tissue. Bars, 50 μm. (B) Graph representing the morphometry results for the mucosa, submucosa, and muscularis of control and infected mouse large intestine. Data show the mean ± SEM. (C) Graph showing goblet cell and enterocyte quantification in the mucosa. Data show the mean ± SEM. Significant differences in the results between the groups for the results shown in panels B ($n = 5$) and C ($n = 12$) were determined by the Mann-Whitney test. *, $P \leq 0.05$. Abbreviations: Mu, mucosa; Mm, muscularis mucosa; Sm, submucosa; M, muscularis; bv, blood vessel; N, nematode; gc, goblet cells; e, enterocytes.

nied by an increase in the mean corpuscular hemoglobin concentration (MCHC) compared with that in the noninfected mice (Table 1). Significant differences in the lipid parameters measured in the serum of infected and control mice were not observed (Table 1), indicating that the nematode infection does not change lipid metabolism or absorption.

Chronic *T. muris* infection induces an increase in the numbers of CD11b$^+$ cells in PPs and MLNs. It was further analyzed whether the chronic nematode infection can induce alterations in Peyer's patches (PPs), mesenteric lymph nodes (MLNs), and spleen (SPL). Infected animals presented an increase in the mass of MLNs and SPL (Fig. 3A), whereas a significant increase in the number of cells was observed only in MLNs (Fig. 3B). These results indicate that *T. muris* infection induces hypertrophy and hyperplasia of MLNs and hypertrophy of the SPL. No differences in the weights of or total cell number in PPs were identified between the control and the infected mice (Fig. 3A and B).

The MLN and PP phenotyping revealed no statistically significant differences in the percentage of CD3$^+$ lymphocytes (Fig. 4), but an increase in the percentage of CD11b$^+$ cells in infected mice compared with that in control mice was found, indicating that the

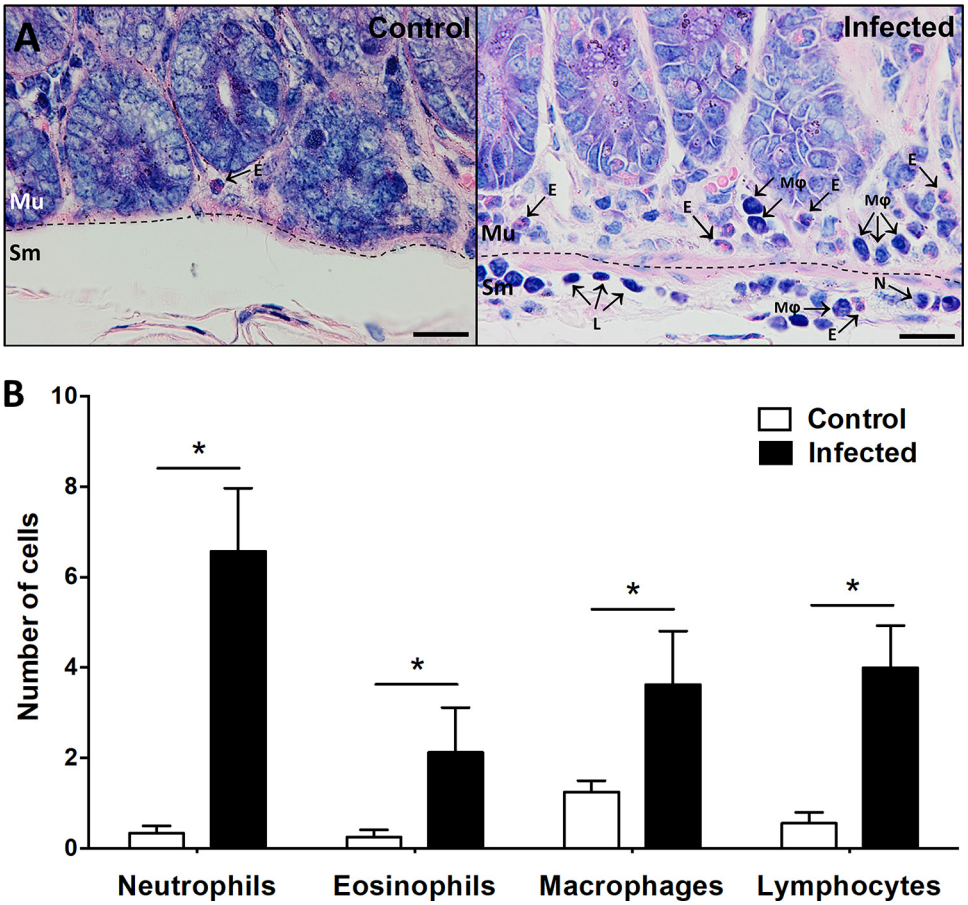

FIG 2 Histological section of large intestine (cecum) stained with Giemsa, showing the cell morphology present in the mucosa and submucosa. (A) (Left) Control tissue without cellular infiltrate. The mucosa and submucosa have rare cells inside. (Right) In infected tissue, it is possible to identify and quantify the cells present in the mucosa and submucosa forming a cellular infiltrate. Bars, 20 μm. (B) Graph showing the results of identification and quantification of the cells present in the submucosa of control and infected animals. Data show the mean ± SEM. Significant difference between the groups were determined by the Mann-Whitney test. *, $P \leq 0.05$ ($n = 5$). Abbreviations: Mu, mucosa; Sm, submucosa; E, eosinophil; N, neutrophil; L, lymphocyte; Mϕ, macrophage.

chronic infection increased the percentage of natural killer, monocytes, macrophages, and/or neutrophils in these organs (Fig. 5A and B), and more details were exhibited by flow cytometry (Fig. 6).

***T. muris*-infected mice exhibited higher levels of Th1, Th2, and Th17 cytokines in mesenteric lymph nodes and serum but not in large intestine tissue than control mice.** To better characterize the immune response in a chronic *T. muris* infection, the levels of Th1, Th2, and Th17 cytokines were measured in three different anatomical locations of the control and the infected mice. Both the MLNs and serum of infected mice presented a significant increase in the levels of the Th1-type cytokines gamma interferon (IFN-γ), interleukin-6 (IL-6), IL-1β, and tumor necrosis factor alpha (TNF-α) and the Th2-type cytokines IL-10 and IL-4 as well as IL-17 compared with those seen in the MLNs and serum of the control animals (Fig. 7A and B). The level of IL-2 was augmented in MLNs and serum, but the increase was statistically significant only in MLNs (Fig. 7A and B). However, an increase in IFN-γ levels was observed only in homogenates of the large intestines of the infected mice and not in those of the noninfected mice, with no differences in the levels of the other cytokines tested being seen (Fig. 7C).

To check the activation state of the immune cells in chronically infected mice, leukocytes were isolated from the mouse peritoneal cavity. The number of total cells isolated from the infected mice was significantly higher than the number isolated from

TABLE 1 Hematological and biochemical parameters of control mice and mice infected by *T. muris*

Parameter[a]	Value (mean ± SE) for the following group:		*P* value
	Control	Infected	
WBC count (10^3/mm^3)	2.65 ± 0.31	10.66 ± 2.49[b]	0.0007
RBC count (10^6/μl)	10.15 ± 0.21	9.33 ± 0.21[b]	0.0295
HGB concn (g/dl)	14.70 ± 0.43	13.68 ± 0.34	0.0884
Hct (%)	55.22 ± 1.25	49.38 ± 1.44[b]	0.295
MCV (fm^3)	54.42 ± 0.74	52.85 ± 0.46	0.0824
MCH level (pg)	14.48 ± 0.34	14.65 ± 0.13	0.5974
MCHC concn (g/dl)	26.64 ± 0.29	27.74 ± 0.20[b]	0.0191
Platelet count (10^3/mm^3)	1658.80 ± 394.09	1631.88 ± 100.61	0.9363
Iron concn (mg/dl)	265.29 ± 14.46	200.17 ± 22.36	0.0286
Total cholesterol concn (mg/dl)	94.54 ± 3.91	90.55 ± 4.16	0.6442
LDL concn (mg/dl)	56.67 ± 1.45	50.00 ± 10.02	0.8260
HDL concn (mg/dl)	7.50 ± 2.50	16.00 ± 11.00	0.9999
VLDL concn (mg/dl)	21.67 ± 2.33	24.33 ± 5.24	0.7000
Triglyceride concn (mg/dl)	108.67 ± 12.77	123.33 ± 26.08	0.7000
C-reactive protein concn (mg/dl)	0.04 ± 0.003	0.04 ± 0.007	>0.9999
Total protein concn (g/dl)	4.26 ± 0.17	4.33 ± 0.23	0.7893
Glucose concn (mg/dl)	187.86 ± 28.21	100.17 ± 15.58[b]	0.0140

[a]Abbreviations: WBC, white blood cell; RBC, red blood cell; HGB, hemoglobin; Hct, hematocrit; MCV, mean corpuscular volume; MCH, mean corpuscular hemoglobin; MCHC, mean corpuscular hemoglobin concentration; LDL, low-density lipoprotein; VLDL, very-low-density lipoprotein.

[b]Significant differences between the values in each column ($P \leq 0.05$) are indicated. Statistical analysis was by the Mann-Whitney test.

the uninfected mice (Fig. 8A). The isolated intraperitoneal immune cells were then allowed to adhere in a culture dish, and the majority of these were peritoneal macrophages. The lipopolysaccharide (LPS) susceptibilities of the cells isolated from both groups of animals were tested. As observed in Fig. 8B, the intraperitoneal macrophages isolated from infected mice released significantly more nitrite (NO^{2-}) in the extracellular medium when they were stimulated with 1, 10, or 100 μg/ml LPS than cells obtained from the control animals.

Excretory-secretory products derived from *T. muris* have anti-inflammatory properties. The bacillary band of *T. muris* is located in the anterior part of the body, specifically, in the region inserted into host tissue during infection. Because this particularity promotes the direct contact of the parasite bacillary glands with the host

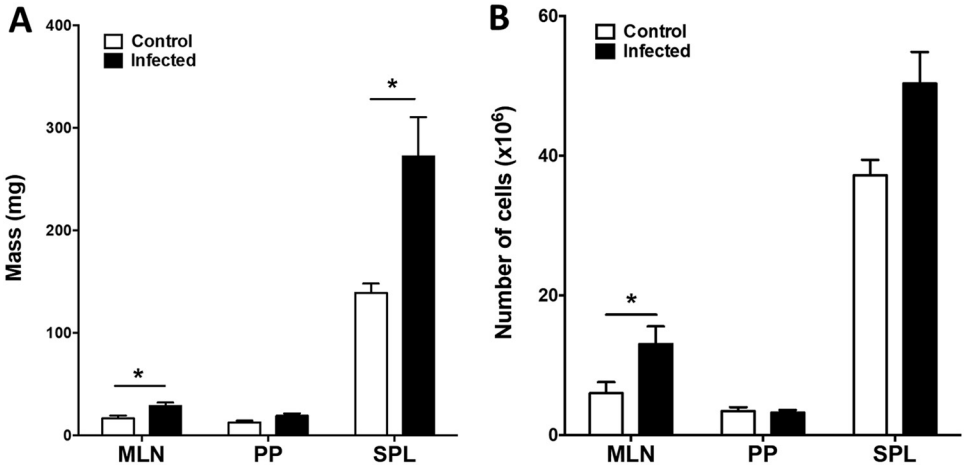

FIG 3 Differences in the mass and cellularity in immune organs from control and infected mice. (A) Mass of the mesenteric lymph nodes (MLNs), Peyer's patches (PPs), and spleen (SPL) isolated from control and *T. muris*-infected mice. (B) Number of total cells in MLNs, PPs, and SPL isolated from control and infected mice obtained by flow cytometry analysis. Significant differences between the groups were determined by the Mann-Whitney test. *, $P \leq 0.05$ ($n = 8$).

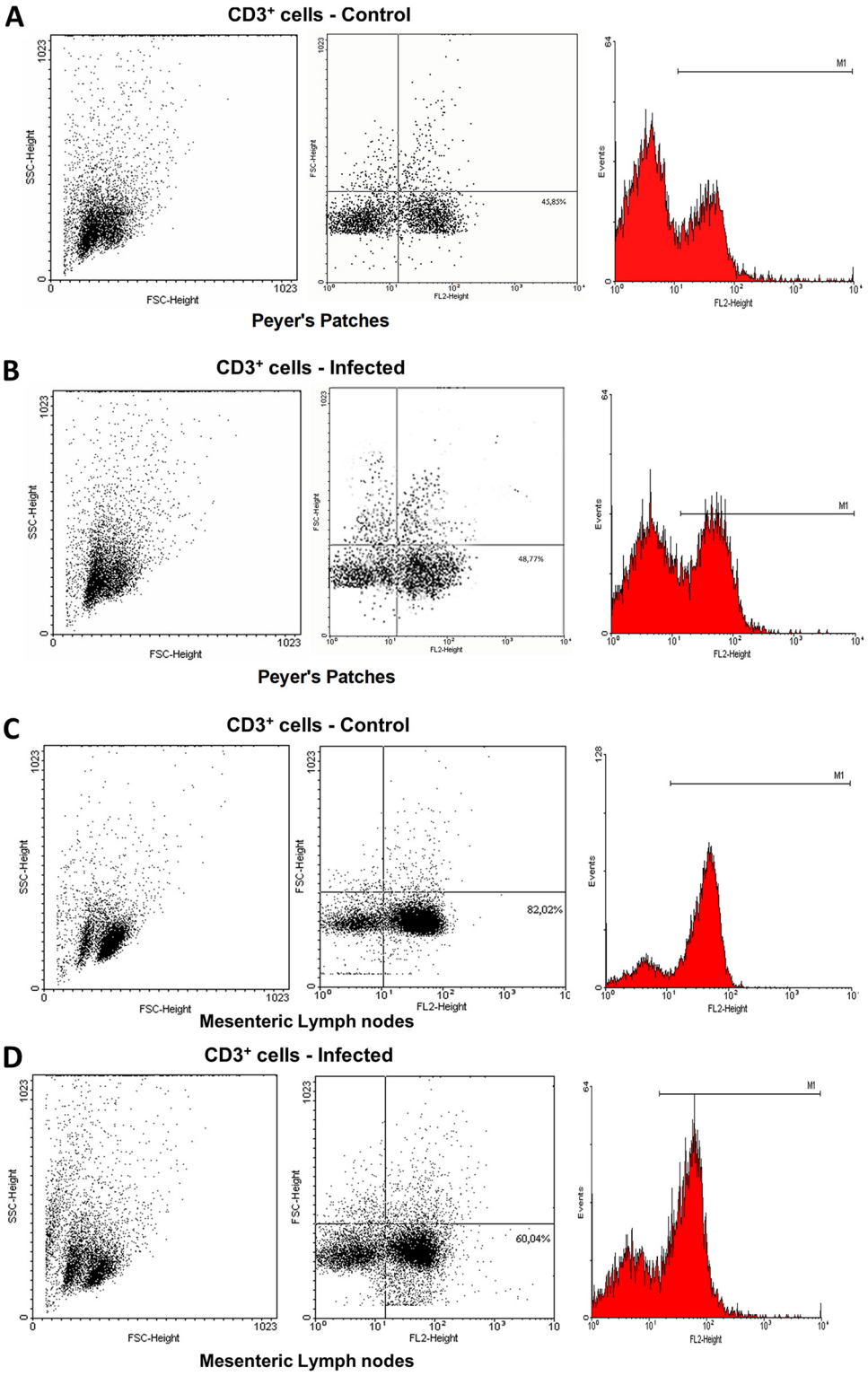

FIG 4 Flow cytometry analysis (dot plot [left] and histograms [right]) of $CD3^+$ cells (fluorescence [FL2] height) from the Peyer's patches of control mice (A), Peyer's patches of infected mice (B), mesenteric lymph nodes of control mice (C), and mesenteric lymph nodes of infected mice (D). The graphs are representative of those from 8 independent experiments. SSC, side scatter; FSC, forward scatter.

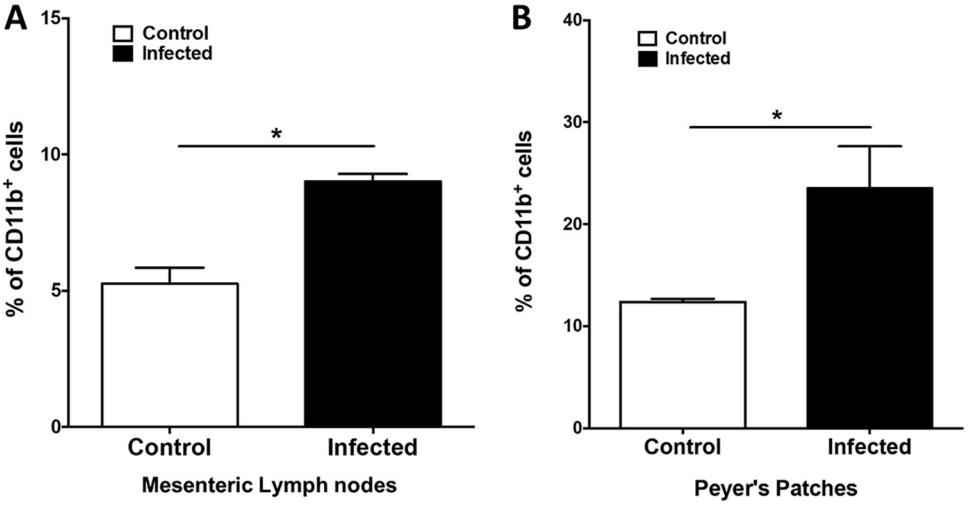

FIG 5 Differences in CD11b$^+$ cell percentages in mesenteric lymph nodes (MLNs) and Peyer's patches (PPs) from control and infected mice. (A) Percentage of CD11b$^+$ cells in MLNs isolated from control and infected mice. (B) Percentage of CD11b$^+$ cells in PPs isolated from control and infected mice. Significant differences between the groups were determined by the Mann-Whitney test. *, $P \leq 0.05$ ($n = 8$).

tissue cells and the inflammatory infiltrate, it was wondered whether the ES products derived from these glands could have anti-inflammatory properties and maybe explain the low cytokine levels detected in the large intestine. To evaluate the effect of ES products from *T. muris*, RAW 264.7 macrophages were preincubated with ES products (10 μg/ml) and subsequently treated with LPS. After that, the amounts of nitric oxide (NO) and two proinflammatory cytokines, IL-1β and TNF-α, released into the culture supernatants were measured. As it is possible to see in Fig. 9A, pretreatment with the ES products from *T. muris* was able to inhibit NO^{2-} production by macrophages treated with LPS (5 and 10 ng/ml). Accordingly, the release of IL-1β and TNF-α, triggered by LPS (100 ng/ml) plus ATP (3 mM), was also inhibited by the pretreatment with the ES products (Fig. 9B and C).

To rule out the possibility that the inhibition of NO and cytokine release observed after pretreatment with the *T. muris* ES product was due to any cytotoxic effect, a viability assay was performed with RAW 264.7 macrophages maintained in culture together with ES products (10 μg/ml) for 24 and 48 h. As expected, the presence of ES products in the culture medium did not have an impact on macrophage viability (Fig. 10).

***T. muris* infection modifies the gut microbiota and promotes bacterial invasion of the intestinal epithelium.** As it was previously shown that *T. muris* infection affects the gut microbiota (19, 20), it was decided to study the bacterial composition in the intestines of mice chronically infected with this nematode. Analysis of fecal cultures of infected and noninfected mice showed a significant increase in the quantity of *Escherichia coli* and members of the *Proteus* genus in infected animals compared with that in control animals (Table 2). In addition, *T. muris*-infected mice exhibited large amounts of *Bacteroides* in their feces, but this genus could not be detected in the feces of the noninfected animals (Table 2). An increase in total anaerobes was observed in *T. muris*-infected mice compared with uninfected mice; however, the difference was not significant.

When the identification of the bacterial species from infected and noninfected mouse feces was performed by matrix-assisted laser desorption ionization–time of flight (MALDI-TOF) mass spectrometry, similar but broad results were obtained for the two groups of mice. The bacterial species *Enterococcus faecalis*, *Enterococcus faecium*, and *Enterococcus gallinarum* were identified only in the infected animals. It was not possible to detect members of this bacterial genus in the uninfected animals. The presence of the bacterial species *E. coli* and *Proteus mirabilis* in both the infected and noninfected groups was also confirmed by MALDI-TOF mass spectrometry (Table 3).

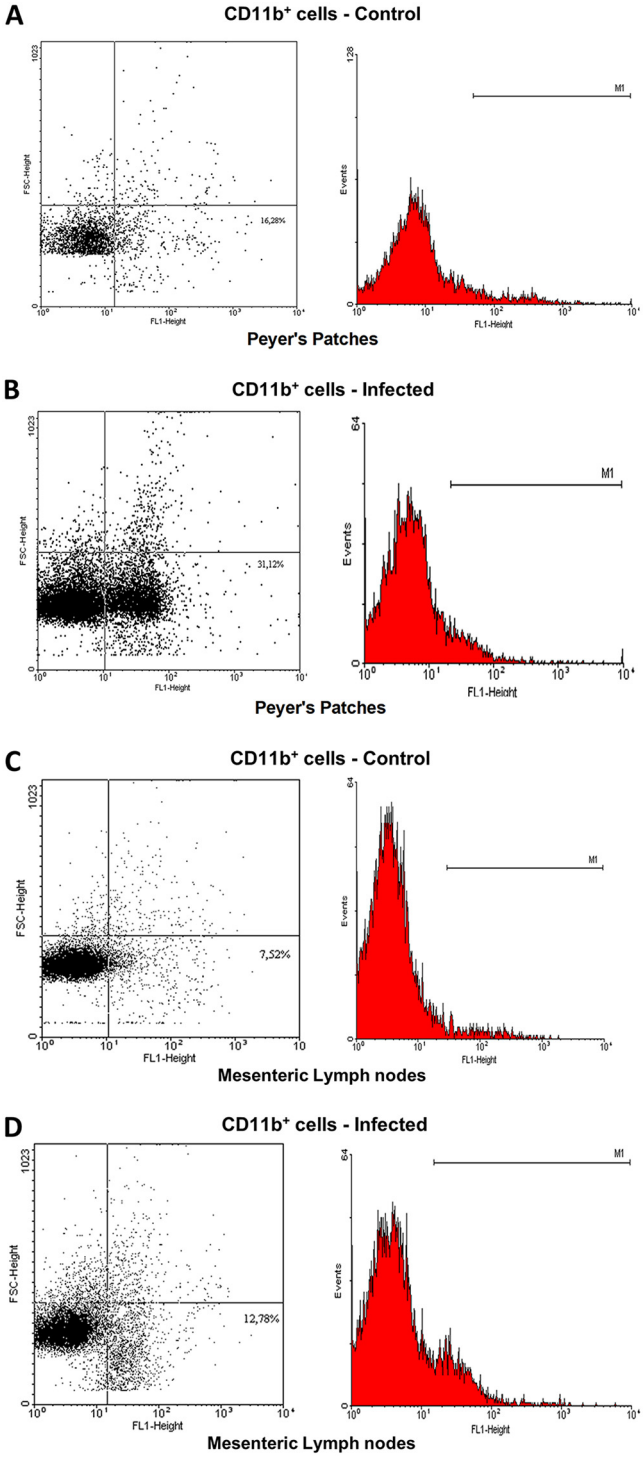

FIG 6 Flow cytometry analysis (dot plot [left] and histograms [right]) of CD11b$^+$ cells (fluorescence [FL1] height) from Peyer's patches of control mice (A), Peyer's patches of infected mice (B), mesenteric lymph nodes of control mice (C), and mesenteric lymph node of infected mice (D). The graphs are representative of those from 8 independent experiments.

Further histological examination of the intestinal mucosa showed that in samples from the control group of mice, bacteria were located only in crypts of Lieberkühn, restricted on the epithelium surface, as expected (Fig. 11A). However, when infected tissues were observed, it was possible to identify bacteria not only in the crypts of

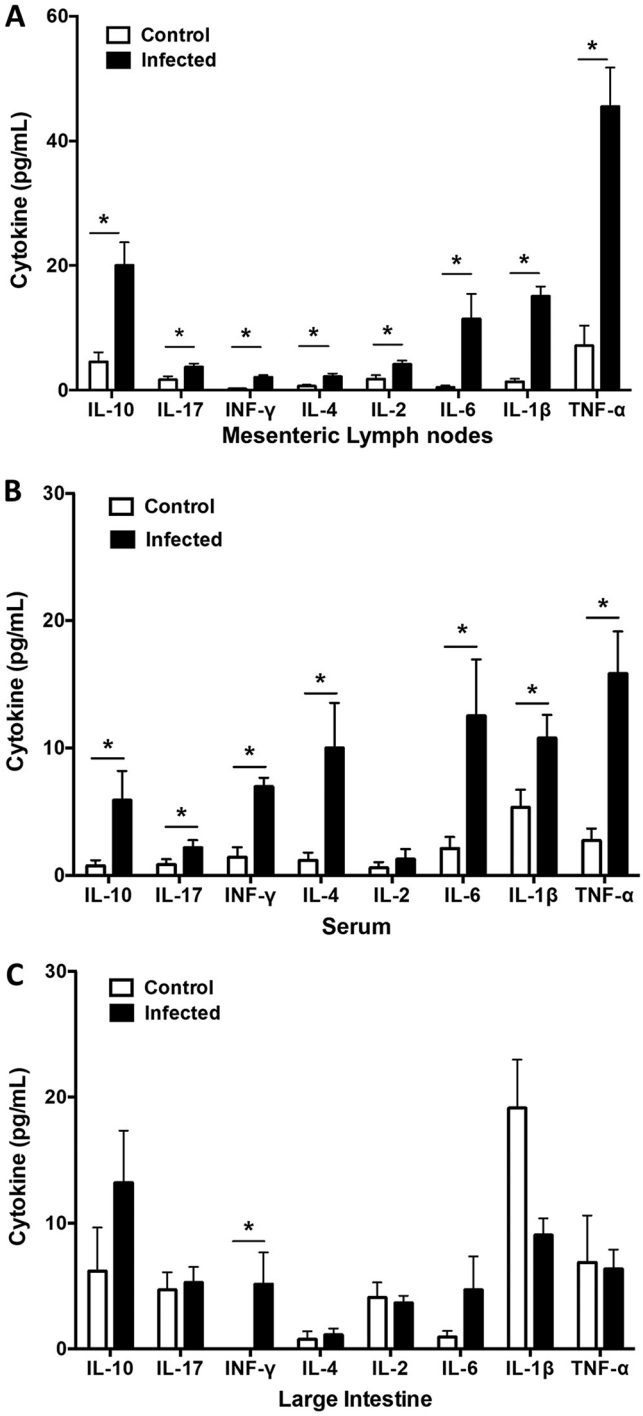

FIG 7 Cytokine secretion in mesenteric lymph nodes, serum, and large intestine of control and *T. muris*-infected mice. After isolation and homogenization, the amounts of cytokines in mesenteric the lymph nodes (A), serum (B), and large intestine fragment (C) were measured using an ELISA kit. Significant differences between the groups were determined by the Mann-Whitney test. *, $P \leq 0.05$ ($n = 8$).

Lieberkühn but also inside the submucosal layer (Fig. 11A, bottom). Using Giemsa stain, the presence of cocci and bacilli was detected in the large intestine submucosa obtained from the infected animals (Fig. 11B and C).

Two different experiments using fluorescence microscopy were performed to obtain evidence of the presence of bacteria. In the first one, intestinal slices from the control and infected mice were stained with DAPI (4′,6-diamidino-2-phenylindole), and it was

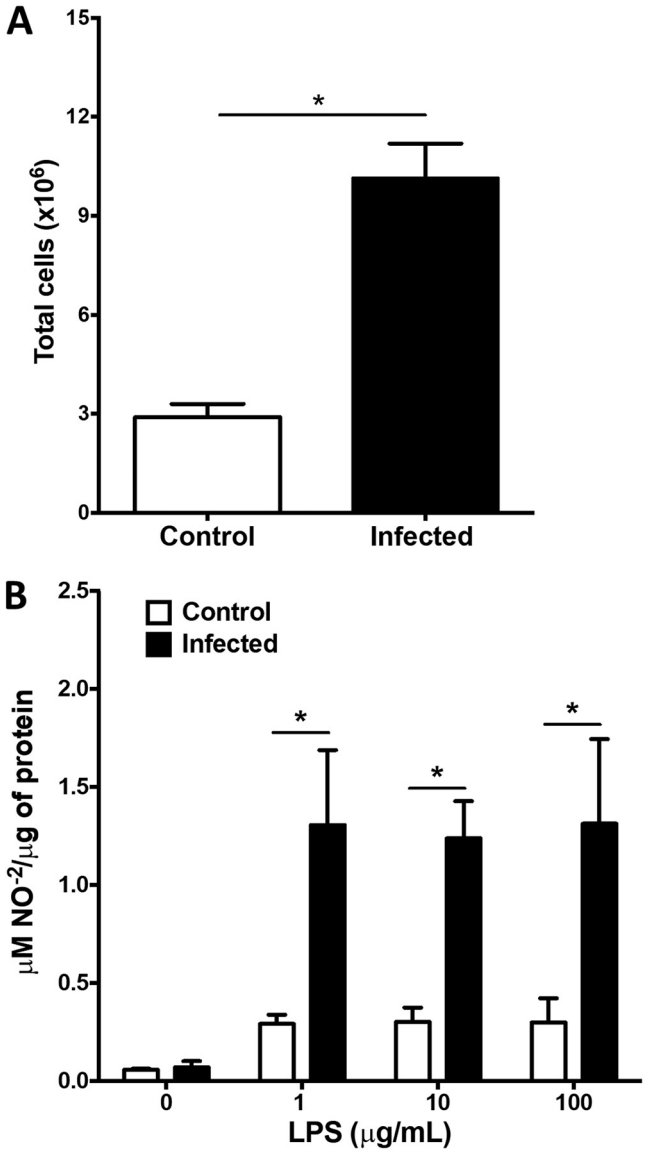

FIG 8 Measurement of the total number of peritoneal cells and NO^{2-} production by macrophages of mice infected or not with *T. muris*. (A) Peritoneal cells from control and infected mice were quantified using a Neubauer chamber. (B) Cultures of peritoneal macrophages from mice infected or not with *T. muris* were maintained under culture conditions for 3 to 5 days and stimulated with LPS (1, 10, or 100 μg/ml) for 24 h. The supernatant was collected and analyzed for the NO^{2-} concentration using the Greiss method. The nitrite concentration was related to the amount of protein in each well, obtained by the Bradford assay after cell lysis. Data show the mean ± SEM from four independent experiments with four mice per group in each experiment. Significant differences between the groups were determined by the Mann-Whitney test. *, $P < 0.05$.

possible to observe a large number of bacilli near the anterior nematode region (Fig. 12A and B), suggesting that the epithelial damage caused by the nematode promotes bacterial invasion. The invasive process was confirmed by fluorescent *in situ* hybridization (FISH) experiments, where it was observed that, in the cecum of mice from the control group, the bacteria (green) were present only in the mucosa layer and were localized in the crypts of Lieberkühn (Fig. 12C and D), whereas in samples from infected mice, the bacteria were identified inside the submucosa (Fig. 12E and F).

DISCUSSION

Whipworms show an unusual biological niche, living for long periods inside the host's intestinal epithelium, often without causing an excessive pathology. The intimate

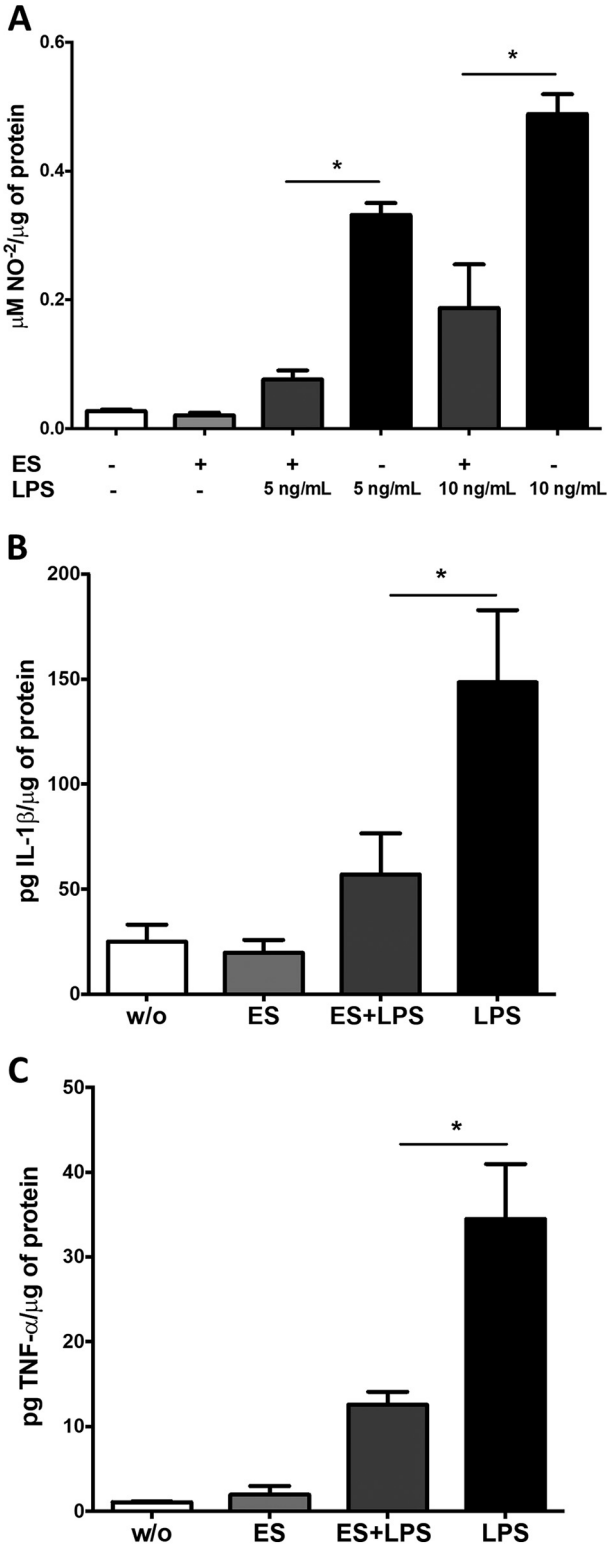

FIG 9 Effect of ES products treatment on NO^{2-}, IL-1β, and TNF-α production in RAW 264.7 macrophages stimulated with LPS. (A) RAW 264.7 macrophages were treated with ES products (10 μg/ml) for 24 h and then stimulated with LPS (5 or 10 ng/ml) for more 24 h. The amount of NO^{2-} in the supernatant was measured using the Greiss method, and the concentration was related to the amount of proteins. (B and C) RAW 264.7 macrophages were treated with ES products (10 μg/ml) for 24 h and then stimulated with LPS (100 ng/ml) for 6 h and ATP (3 mM) for an additional 2 h. The IL-1β (B) or TNF-α (C) concentration in the supernatant was measured using the appropriate ELISA kit, and the concentration was related to the amount of proteins. Data show the mean $\pm$ SEM from four independent experiments. Significant differences between the groups were determined by the Mann-Whitney test. *, $P < 0.05$ ($n = 5$).

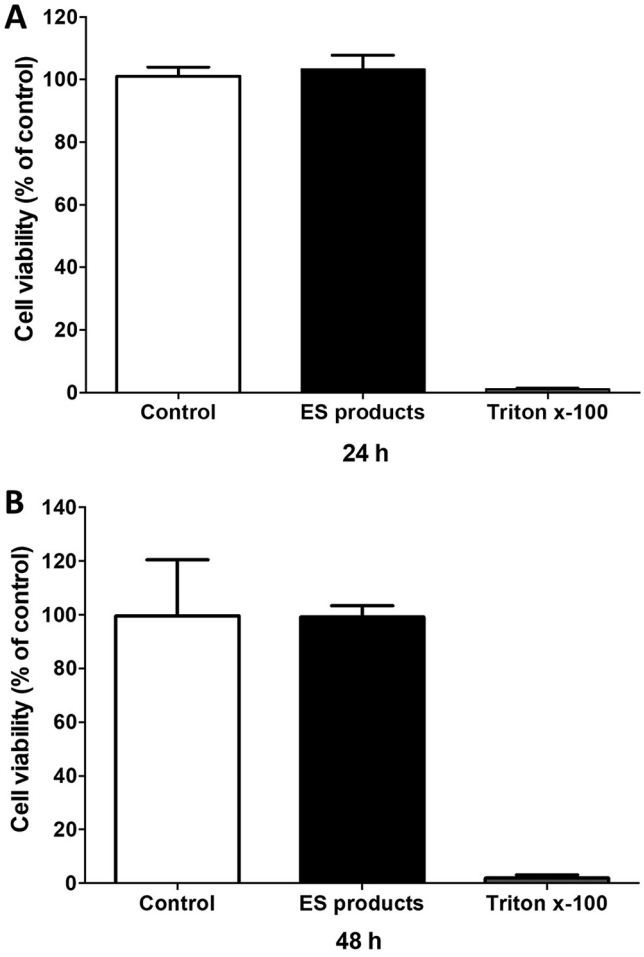

FIG 10 Effect of *T. muris* ES products on the viability of RAW 264.7 cells. Cells were exposed to ES products (10 μg/ml) for 24 h (A) and 48 h (B), and then cell viability was measured using the MTT assay. Untreated macrophages (culture medium) were considered 100% viable, and lysed macrophages were used as a positive toxicity control. The percentage of macrophages in culture medium plus *T. muris* ES products (10 μg/ml) was expressed in relation to the value for the control (100%). Data show the mean ± SEM from three independent experiments.

contact of the nematode with host tissues and microbiota requires specific adaptations, such as the secretion of immunomodulatory factors by the parasite. While most of the pathological studies have examined the acute immune response to *T. muris* and the balance between resistance and susceptibility to infection (8, 12, 24–26), only recently a growing number of works have analyzed the animals' immunopathological processes during chronic infection (18–20, 27–30). Normally, outbred mouse strains show similar proportions of susceptible individuals and individuals resistant to infection. Outbred

TABLE 2 Analysis of bacteria in feces by biochemical tests

Species	No. of CFU (mean ± SE)		*P* value
	Noninfected mice	Infected mice	
Total anaerobes	$(7.9 \pm 3.2) \times 10^5$	$(8.02 \pm 2.0) \times 10^6$	0.1508
Bacteroides	ND[a]	$>10^7$	ND
E. coli	$(2.6 \pm 0.8) \times 10^3$	$(1 \pm 0.07) \times 10^{5}$[b]	0.0022
Enterococcus	$>10^7$	$>10^7$	ND
Proteus	$(1.9 \pm 1.9) \times 10^4$	$(5.3 \pm 2.4) \times 10^{5}$[b]	0.0317

[a]ND, not detected.
[b]Significant differences were found for *E. coli* ($P = 0.0022$) and for *Proteus* spp. ($P = 0{,}0317$). Statistical analysis was by the Mann-Whitney test.

TABLE 3 Identification of bacterial species in feces using MALDI-TOF mass spectrometry

	Noninfected mice		Infected mice	
Bacterial species	**Present**	**Score[a]**	**Present**	**Score**
Enterococcus faecalis			X	2.207
Enterococcus faecium			X	2.468
Enterococcus gallinarum			X	2.055
Escherichia coli	X	2.303	X	2.128
Proteus mirabilis	X	2.23	X	2.314

[a]Scores were for the species level (score ≥ 2) and genus level (score ≥ 1.7). The scores for all strains were determined in duplicate.

strains display a genetic variability that is closer to conditions in nature than that seen for inbred strains. Both humans and wild-type animals are susceptible to infection, with individual immunosuppressive conditions favoring susceptibility and the establishment of a chronic infection (31–33). It was decided to use an outbred mouse strain with induced tolerance to infection because it was considered that such a model must approximate the situation in the human colon during chronic trichuriasis (34).

A significant thickening was detected in the three layers of the large intestine in mice chronically infected with *T. muris*. Hyperplasia and hypertrophy of goblet cells were also observed in the infected animals compared with the findings for the control group. These results are in agreement with the data shown by others (35), obtained using an experimental model of C57BL/6 mice infected with *Nippostrongylus brasiliensis*. In this model, the infected animals also showed intestinal goblet cell hyperplasia (35), and recently, the epithelial hyperplasia observed in C57BL/6 mice chronically infected with *T. muris* was associated with cancer development (20). On the other hand, other groups did not find differences in the numbers of goblet cells or alterations in the thickening of the large intestine layers in C57BL/6 mice infected by *T. muris* at 35 days compared with the findings for control mice (36). The dissimilar findings may reside in the distinct genetic backgrounds of the mouse strains or infection times, because the analysis in this study was conducted on day 45, while the study of Ramanan and coworkers (36) was conducted on day 35.

Protein malnutrition is a clinical condition reported in infections caused by soil-transmitted helminths, including trichuriasis (37). In this work, no differences in the quantities of enterocytes between the control and the infected mice were observed; however, histopathological studies showed that malnourished children with persistent diarrhea present a positive relationship between the degree of malnutrition and the decrease in the size of enterocytes and their nuclei (38). The impact of trichuriasis on enterocyte biology is an important issue in human and veterinary health that remains to be revealed.

The parasitism lesions developed by *T. muris* in this experimental model promoted an infiltrate in the submucosa with increased number of neutrophils, eosinophils, macrophages, and lymphocytes. Eosinophilic infiltration was also described in biopsy specimens from patients with trichuriasis in South Korea (39). A similar mucosal cell infiltrate was registered in the C57BL/6 mouse model of chronic *T. muris* infection (20), and a large influx of macrophages into the large intestine of infected BALB/c and AKR mice was also reported (24).

It was shown that the chronic phase of *T. muris* infection produces alterations in hematological and biochemical parameters. One remarkable alteration in hematological values was the significant increase in the numbers of the leukocytes in infected mice, which probably indicates an immunological response to the tissue damage and bacterial invasion (see below). A significant reduction in the number of red blood cells as well as in the hematocrit percentage was observed, as was a slight, but not significant, decrease in the iron content in the blood of the infected animals, which may indicate iron deficiency anemia. Similar results were obtained in humans infected with *T. trichiura* (40, 41), and a study showed that C57BL/6 mice infected with a low dose of *T. muris* eggs did not have anemia (28), suggesting that the parasitic load directly

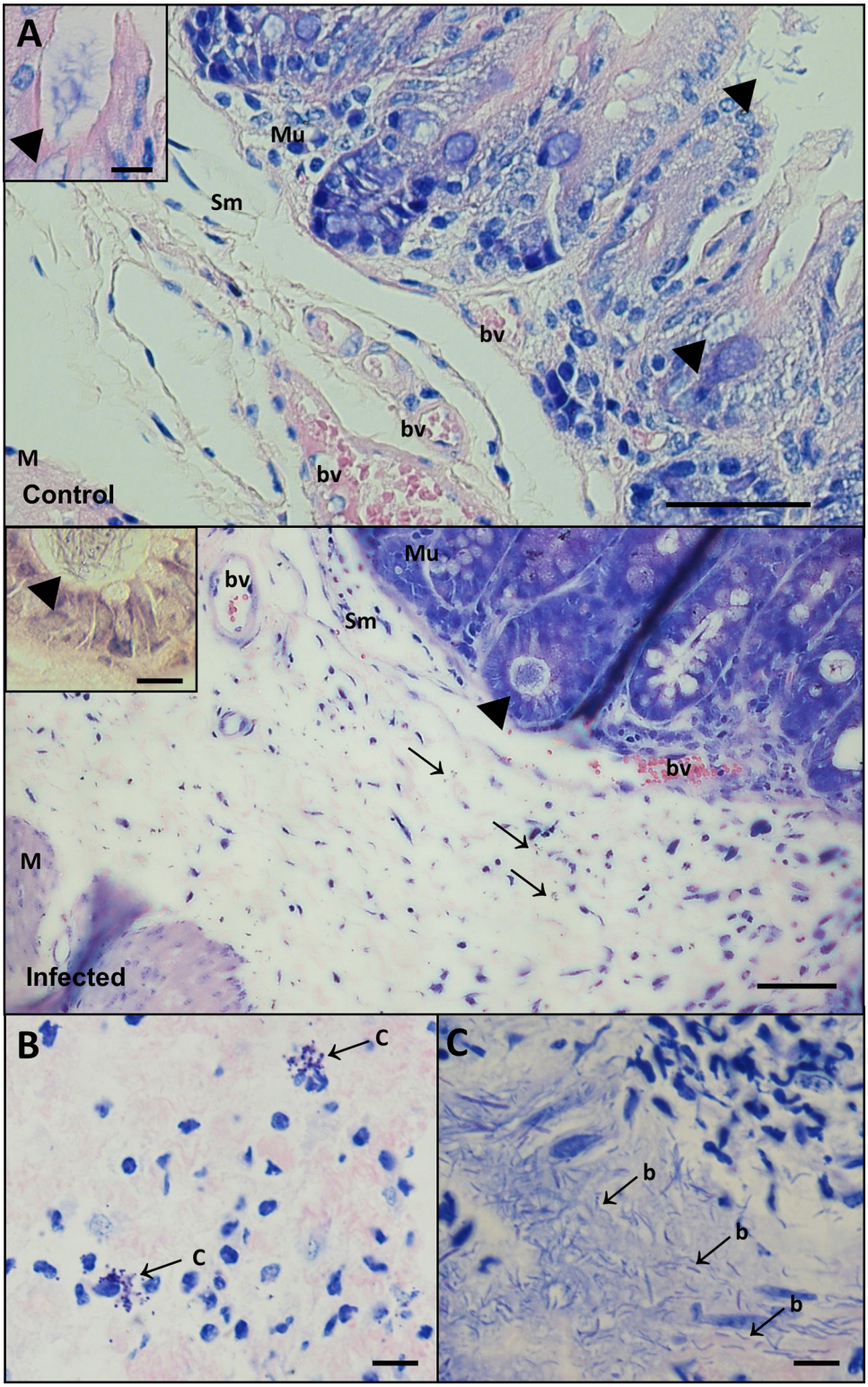

FIG 11 Histological sections of large intestine (cecum) stained with Giemsa for analyses of bacterial invasion in the submucosa layer. (A) (Top) Control tissue with bacteria in the intestine lumen and inside the crypt of Lieberkühn (arrowhead). (Inset) Detail of the control tissue showing bacilli in the crypt of Lieberkühn (arrowhead). (Bottom) Infected tissue with bacteria inside the crypt of Lieberkühn (arrowhead) and invasive bacteria (arrow) in the submucosa layer. (Inset) Detail of the infected tissue showing bacilli in the crypt of Lieberkühn (arrowhead). Bars, 50 μm. Inset bars, 10 μm. (B) Submucosa with invasive coccus-shaped bacteria, lymphocytes, and macrophages. Bar, 10 μm. (C) A large number of the invasive bacilliform bacteria in the submucosa, neutrophils, and eosinophils were also identified. Bar, 10 μm. The data in panels B and C are representative of those from 5 experiments. Abbreviations: c, coccus-shaped bacteria; b, bacilliform bacteria; Mu, mucosa; Sm, submucosa; bv, blood vessel; M, muscularis.

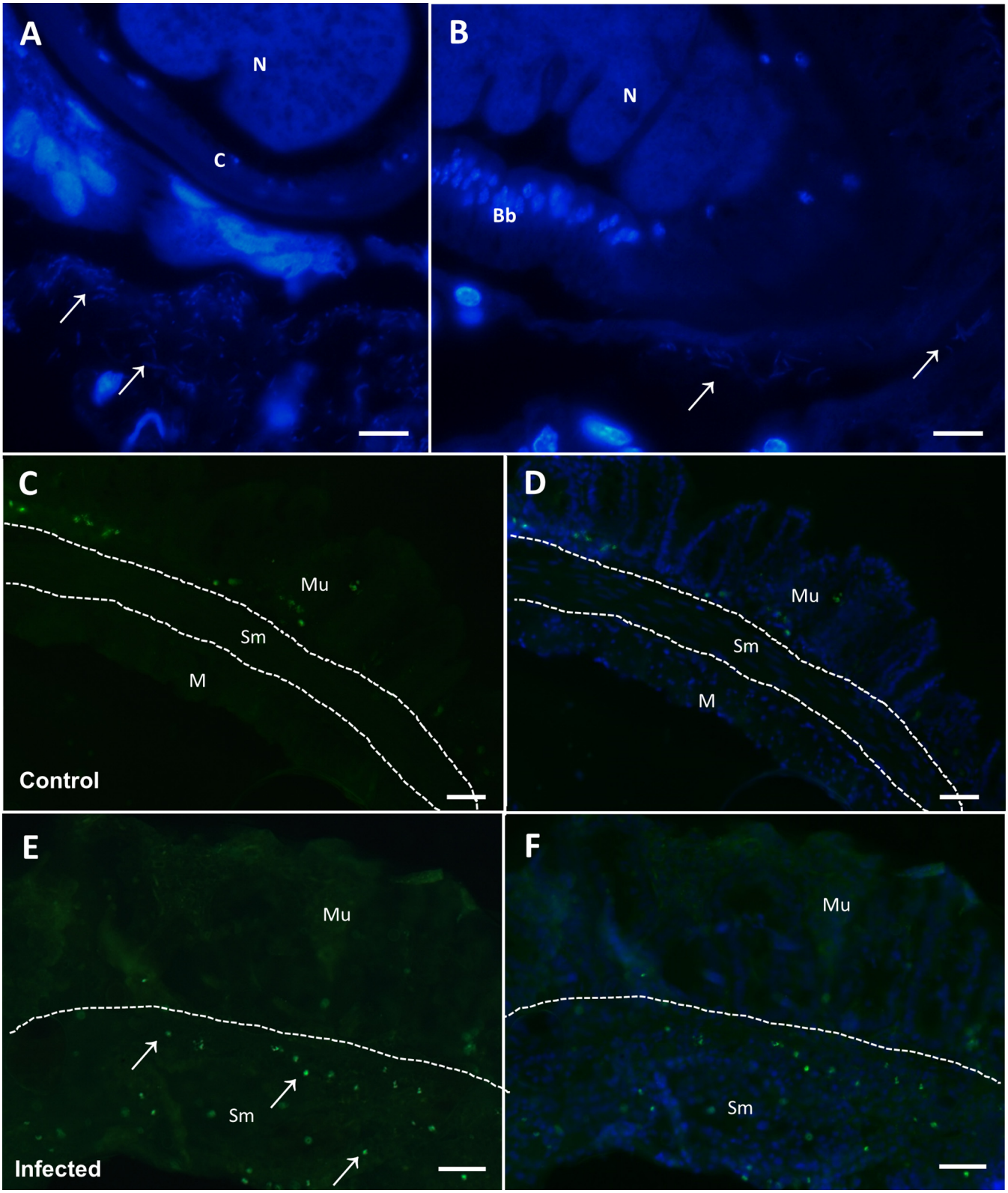

FIG 12 Fluorescence microscopy, using DAPI and fluorescence *in situ* hybridization (FISH), of sections of control and infected tissues showing bacterial invasion. (A and B) DAPI experiments showing the anterior region of the nematode inserted in the intestinal tissue and bacilliform bacteria (arrows) close to the nematode cuticle. In panel B, it is possible to identify the bacteria (arrows) and the bacillary band of the *T. muris* nematode. (C and D) FISH experiments showing the three layers of the uninfected cecum tissue and the bacteria (green) present only in the mucosa. (E and F) FISH experiments showing infected tissue invaded by bacteria (green) in the submucosa (arrows). (D and F) Merged figures showing bacteria (green) and host tissue (DAPI). Bars, 10 μm (A and B) and 50 μm (C to F). The images are representative of those from 5 experiments. Abbreviations: N, nematode; c, cuticle; Bb, bacillary band; Mu, mucosa; Sm, submucosa; M, muscularis.

impacts the hematocrit. These results show that outbred animals, such as Swiss Webster have a heterogeneous response more similar to that seen in human infections than that seen in infections in isogenic mice.

The weight loss observed in the infected animals in the present study may have been related to the glucose deficiency in the blood. Previous *in vitro* experiments showed that the *T. muris* bacillary band, the nematode region inserted into the host tissue during parasitism, accumulates and absorbs glucose (15). In addition, our results showed that the infection promotes bacterial invasion and a significant increase in the numbers of anaerobes and *E. coli* bacteria in the intestine. It seems possible that alterations in the microbiota also modify carbohydrate metabolism, as was described before in the case of pigs infected with *T. suis* (9).

A significant hypertrophy of the MLNs and SPL of mice chronically infected with *T. muris* was observed; however, hyperplasia was detected only in the MLNs, the lymph nodes draining the large intestine. Greater numbers of macrophages were observed in the mucosa of resistant mouse strains than in the mucosa of susceptible strains (24), suggesting a key role for these cells in infection. Phenotypic characterization showed a higher proportion of $CD11b^+$ cells in the MLNs and PPs, indicating that monocytes, neutrophils, natural killer cells, granulocytes, and/or macrophages migrate to regions close to the parasite location as a consequence of the infection. Increased numbers of $CD11b^+$ cells in MLNs were also described before in a C57BL/6 mouse model of *T. muris* infection (26). PPs and MLNs are the two main sites where immune responses against intestinal pathogens can be initiated; however, data about *T. muris* infection are still limited at present.

The type of immune response generated against *T. muris* during the first days of infection determines the balance between susceptibility and resistance to infection. A Th2-type response is associated with parasite expulsion, whereas a Th1-type response is associated with the establishment of a chronic infection (12). However, characterization of the immune response using murine models with 45 days of infection is rare, despite the fact this condition could be closer to the situation in humans with long periods of parasitism. In the study described here, the amounts of responses of the Th1, Th2, and Th17 types were increased in the MLNs, PPs, and serum of infected mice compared with those of the uninfected animals, compatible with a mixed immune response. In the large intestine, only the levels of IFN-γ in infected mice were significantly higher than those in the control mice, with no differences in the amounts of the other cytokines measured being seen. The depletion of IFN-γ in susceptible AKR mice resulted in expulsion of the parasite (23), suggesting an important role of this Th1 cytokine in the maintenance of a chronic infection. The treatment of normally resistant BALB/K mice with an anti-IL-4 receptor antibody resulted in a chronic *T. muris* infection (23), showing that IL-4 participates in parasite expulsion. Under the conditions used in this study, the levels of IL-4 remained low in the large intestine and IFN-γ was the only Th1 cytokine present at significantly larger amounts in the large intestine of infected mice than in that of the control mice, maintaining an environment where the parasite could be detected in the host. The levels of IFN-γ in cultures of MLNs from AKR mice chronically infected with *T. muris* were higher than those in uninfected mice (27) and were also higher than the levels produced by the same cell type isolated from resistant BALB/c mice (26), showing that the level of this Th1-type cytokine is elevated during the development of infection, in agreement with our results. $CD4^+$ T cells from the colons of *T. muris*-infected C57BL/6 mice displayed an increase in IFN-γ production when they were isolated and stimulated with phorbol myristate acetate and ionomycin in the culture compared with that for cells from noninfected mice (18, 36). Also using C57BL/6 mice, Chenery and coworkers showed that a chronic infection with *T. muris* causes IFN-γ-expressing T-cell accumulation in the bone marrow, demonstrating a Th1 cell-driven response to infection (28). However, up to now there have been no records of studies covering the several cytokine classes that were measured in this work at 45 days of chronic *T. muris* infection in three different tissues. In schistosomiasis and filariasis, it was observed in individuals with a chronic pathology that the parasite causes a

damaging immunopathology, with high levels of Th1-, Th2-, and Th17-type cytokines being found in serum (42). Reinfection with *Fasciola hepatica* potentiates a mixed Th1/Th2/Th17/regulatory T cell response in Wistar rats (43). A mixed Th1/Th2 cytokine response was also observed in mice treated with *Taenia solium* metacestode antigens (44). Intestinal gene expression in pigs infected with *T. suis* showed an increased expression of genes for the Th1-type cytokines IL-1α and IL-6, as well as genes involved in the release of the Th2-type cytokine IL-13 (45). Besides, it seems logical to think that the immune state of the whole individual after 45 days of infection is a mix of not only the immune response elicited by the nematode parasite antigens but also the immune response induced by the bacterial invasion resulting from rupture of the intestinal epithelial barrier as well as the inflammation that occurs as a consequent of the tissue damage itself.

Surprisingly, the amounts of cytokines in the large intestine showed no difference between infected and control mice (with the exception of IFN-γ), despite the fact that a massive infiltrate with large amounts of macrophages in the submucosa was observed. This fact leads us to wonder about the macrophage activation state in the infected mice. It was found that the number of intraperitoneal cells, mainly monocytes and neutrophils, recruited during infection was significantly higher in the infected group than in the control group, suggesting peritonitis. In addition, the differentiated macrophages isolated from infected mice were more responsive to LPS treatment than those isolated from uninfected mice, indicating that these cells are in an activated state.

It has been known for a long time that helminths secret products that can interact with the host, and immunomodulatory activity has been found in the ES products of several species of parasitic worms (16). Recently, two different groups characterized the ES products of *T. muris* and identified more than 100 proteins and 20 microRNAs (17, 46). Little is known about the effects of ES products from *T. muris* on immune cells. D'Elia and Else showed that the ES products from *T. muris* stimulate the secretion of IL-10 and IL-6 from bone marrow-derived macrophages and dendritic cells (47). It was shown here, for the first time, that the ES products of this nematode inhibit the inflammatory response of macrophages stimulated with bacterial LPS. This could be the explanation for the low levels of cytokines found in the large intestine, where the worm is in close contact with the host and the ES products can have potent immunomodulatory effects.

The intestinal microbiota contributes to nutrient digestion and absorption and also modulates the individual immune response. Trichuriasis can promote an imbalance in these functions, since the parasite can affect the microbiota composition. Swine infected with *T. suis* present changes in their microbiota (22), and this could be related to the decrease in carbohydrate metabolism and amino acid biosynthesis observed in parasitized animals (9). It was previously shown that *T. muris* infection decreases the diversity of the microbiota, increasing the abundance of members of the *Lactobacillus* genus (19), and that the alterations in the microbiota composition can be reversed after clearance of the infection (20). In agreement with these findings, in the present study, it was shown that *T. muris* infection promotes a significant increase in total anaerobes, with a dramatic increase in the numbers of *Escherichia coli* bacteria and *Bacteroides* spp. MALDI-TOF mass spectrometry confirmed the results of the biochemical tests for *E. coli* and *Proteus* and identified three different species of *Enterococcus*. A similar increase in the abundance of *Bacteroides* spp. was also described in C57BL/6 mice chronically infected with *T. muris* (19, 20) and in pigs infected with *T. suis* (9). In a report describing findings different from those described above, Ramanan and coworkers reported that chronic *T. muris* infection inhibits *Bacteroides vulgatus* colonization and promotes the establishment of a protective microbiota enriched in the *Clostridiales* (36). In the same work, the authors described no differences in corporal weight or morphological alterations between the intestines of infected C57BL/6 mice and those of uninfected mice (36). A finding that may explain the discrepancies in the results obtained by these different research groups comes from a recent study that compared the immune response and the microbiota changes induced by chronic infection with *T. muris* in

C57BL/6 mice maintained under controlled laboratory conditions or in an outdoor environment (48). The mice placed in an outdoor environment that was similar to their natural habitat harbored larger worm biomasses than the laboratory mice and also showed decreased Th2-type and increased Th1-type immune responses, with higher levels of inflammatory cytokines being seen in the intestine and MLNs (48). These interesting results indicate that the interactions between the host and the nematode are strongly affected by the genetic background and the environment, the latter of which also affects the diet. Changes in diet can affect the microbiota; in addition, changes in the microbiota can shape the immune response. As a consequence of all these interactions, the immune state during a helminth infection is the result of the cross talk of all these factors in each individual host. In humans, the data related to microbiota changes induced by trichuriasis also conflict. The composition of the microbiota in children from Ecuador infected with *T. trichiura* did not show significant differences from that in uninfected children (49). On the other hand, an indigenous population in Malaysia infected with helminths showed a reduction in the alpha diversity of their microbial communities after treatment with albendazole, indicating that the parasite probably increases the diversity of the microbiota (50). Once more, it is expected that differences in geographic location, diet, genetic background, age, and gender may lead to different results among studies.

Because the adult worm promotes tissue rupture, forming syncytial tunnels (6), several authors hypothesized that these disruptions in the mucosa may allow the entrance of cecal bacteria (6, 29, 51). In this work, invading bacteria were identified in the large intestine (cecum) submucosa of *T. muris*-infected mice. These lesions on the intestinal tissues serve as a means of access for the lumen bacteria and may promote aggravation of the pathology. The presence of bacteria inside the host tissues could be responsible for the mixed Th1/Th2/Th17 profile observed in infected mice. It was hypothesized that macrophages in the mucosa and submucosa in close contact with bacteria maintain a slow production of proinflammatory cytokines due to the secretion of products from the nematode. This seems to be an evolutionary strategy to avoid a deleterious inflammatory response that could be harmful to the parasite, as well as to the host. It is important to note that no bacteria were identified in the muscularis layer of the large intestine or in the bloodstream, suggesting that immune cells in the submucosa prevent the spread of these microorganism by the host body. More experiments should be carried out to elucidate the association of these invasive bacteria with the nematode infection process and with the host's inflammatory state.

The evolution of the mammalian immune system happened in intimate association with the establishment of helminth parasitism in metazoans (52). Complex mechanisms in the relationship among the host immune response, the gut microbiome, and parasite survival strategies are involved. These three players participate in the host health state, and an understanding of this cross talk is fundamental to understand the clinical evolution of this infection and think about new therapeutic strategies. This study contributes, for the first time, new data from a model with an outbred mouse strain. Alterations in the intestinal tissue, changes in the microbiota composition, and a mixed immune response, probably resulting from invasion by intestinal bacteria, together with the effects of the worm and ES products, were described (Fig. 13).

MATERIALS AND METHODS

Ethics statement. The parasite life cycle was maintained in the Otto Wucherer Helminth Biology Laboratory, and all the animal protocols were approved by the Ethics Committee for Animal Experimentation of the Health Sciences Center of the Federal University of Rio de Janeiro under protocol IBCCF 149, according to Brazilian federal law (Law 11.794/2008, regulated by Decree 6.899/2009), based on the *Guide for the Care and Use of Laboratory Animals* (53), prepared by the National Research Council of the U.S. National Academy of Sciences, and the *Australian Code of Practice for Care and Use of Animals for Scientific Purposes* (54). All the animals received humane care in compliance with the above-mentioned guides, used by the Ethics Committee to approve the protocol.

Experimental infections and collection of excretory-secretory products. Eggs from the *Trichuris muris* Edinburgh strain, provided by Francisco Bolas (Universidad Complutense de Madrid), were washed twice in dechlorinated water and incubated at 28 ± 2°C for 45 days. After this period, the percentage of

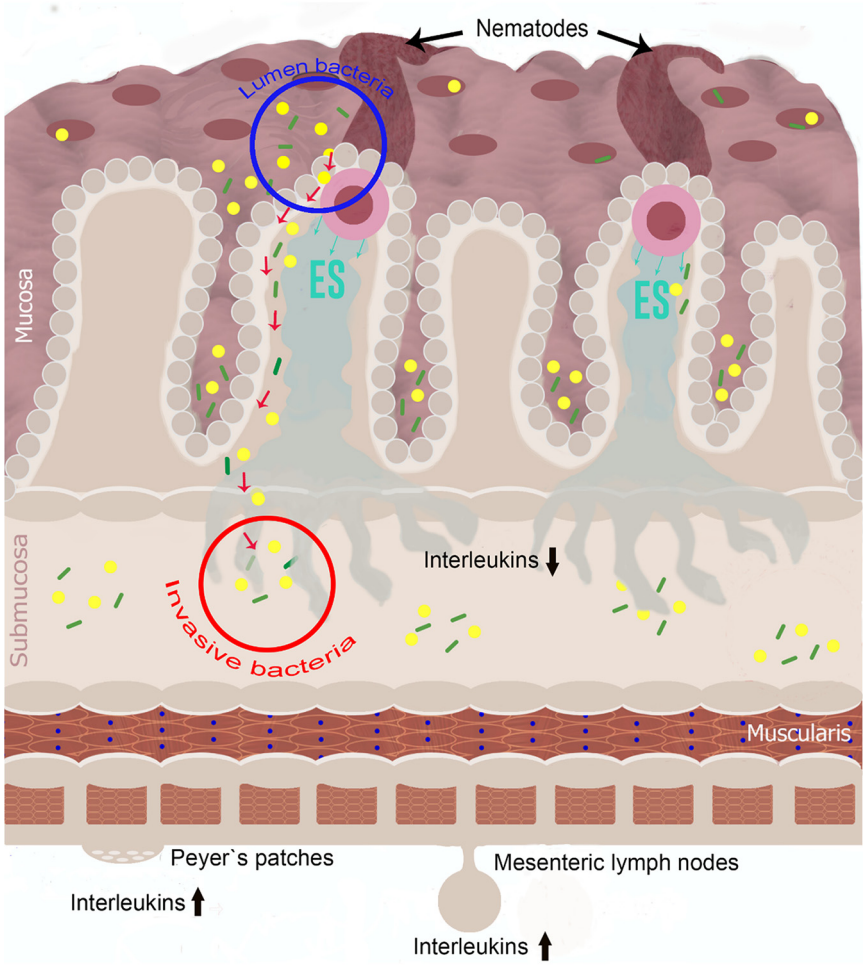

FIG 13 Illustration showing the large intestine (mucosa, submucosa, and muscularis) infected with *T. muris* (nematodes), excretory-secretory (ES) product release (blue arrows), the bacterial invasion process (red arrows), and the immunological response (interleukins). The infographic is a summary of the results of this study showing the tissue damage caused by the nematodes. The damage promotes bacterial invasion into the tissue and modulation of the immunological response as a consequence of ES product secretion. It is possible to identify an increase in the amounts of interleukins in Peyer's patches and mesenteric lymph nodes; however, this was not observed for the interleukins dosed directly in the large intestine (tissue).

embryonated eggs was estimated by light microscopy. Two hundred embryonated eggs in 0.3 ml of dechlorinated water were administered orally to 20 laboratory-bred male Swiss Webster mice aged 4 to 6 weeks, and the control group was administered 0.3 ml of dechlorinated water. Infected and control mice were immunomodulated with 50 μl of dexamethasone sodium phosphate (8 mg/ml) and dexamethasone acetate (10 mg/ml) (Duo-Decacron; Aché Laboratory) at 7, 9, and 11 days postinfection. The immunomodulation has an influence only in the first days of infection (drug half-life, 2 h) and was performed in order to establish a parasitic load in the chronically infected mice. After 45 days of infection, the mice were euthanized (in a CO_2 chamber) and necropsied, and the different tissues were recovered. The health conditions of the experimental mice were evaluated as described previously (55).

For the collection of *T. muris* excretory-secretory (ES) products, adult worms were gently removed from the large intestine tissue (cecum) with the aid of a round brush (no. 4) and immediately transferred into and incubated in 24-well plates with serum-free RPMI 1640 medium containing 2 mM L-glutamine (Gibco) along with 100 U/ml penicillin and 100 μg/ml streptomycin (Sigma-Aldrich) at 37°C in 5% CO_2. After 24 h, the supernatant was collected and maintained overnight in an endotoxin removal column, according to the manufacturer's specifications (Thermo Scientific).

Gut histology: morphometric and morphological experiments. Large intestine fragments taken from the cecum region were fixed in 8% formaldehyde at pH 7.4 for 24 h and transferred to 4% formalin. The tissue was dehydrated in a graded ethanol series (30% to absolute), subjected to diafanization with xylene (Merck), and embedded in paraffin (Sigma-Aldrich). Tissue sections (5 μm) were obtained and stained with hematoxylin-eosin (Sigma-Aldrich), Giemsa (Merck), and periodic acid-Schiff (PAS).

Morphometric and morphological analyses were performed using the software Bel View (version 6.2.3.0; Bel Engineering, Monza, Italy), and images were obtained using a Nikon Eclipse 80i microscope

equipped with a Nikon DS-Ri1 digital camera. The three cecum layers in five different areas in five animals from each group (the control and the infected groups) were measured at random. For morphological experiments in the submucosa, the cells in three areas of 50 μm^2 randomly selected from five animals from each group were quantified and identified. For enterocyte and goblet cell quantification, three crypts of Lieberkühn were randomly selected from four animals from each group and analyzed.

Hematological and biochemical analyses. During the necropsy, cardiac puncture was performed for the collection of blood (0.8 to 1.0 ml) from the infected and the control mice. The blood samples were stored in vials containing EDTA as an anticoagulant for hematological analysis and in microtubes without anticoagulant for biochemical analysis. The samples intended for biochemical analysis were centrifuged at 500 $\times$ *g* for 5 min to obtain serum for the experiments. Altogether, the total leukocyte (WBC) count (in 10^6 cells per microliter), red blood cell (RBC) count (in 10^6 cells per microliter), hematocrit (in percent), hemoglobin (HGB) concentration (in grams per deciliter), mean corpuscular volume (MCV; in femtoliters), mean corpuscular hemoglobin (MCH) amount (in picograms), mean corpuscular hemoglobin concentration (MCHC; in grams per deciliter), platelet count (in 10^6 cells per microliter), iron concentration (in milligrams per deciliter), glucose concentration (in milligrams per deciliter), C-reactive protein concentration (in milligrams per deciliter), total protein concentration (in grams per deciliter), total cholesterol fractions (low-density lipoprotein, high-density lipoprotein, and very-low-density lipoprotein; in milligrams per deciliter), and triglyceride concentration (in milligrams per deciliter) were determined. The samples were evaluated in the Clinical Analyses of Laboratory of Animals platform (RPT12C platform; Fiocruz) and in the Laboratory of Lipids platform (LabLip platform; UERJ), which are certified by the Analytical Quality Control Program of the National Program of Quality Control (PNCQ) of the Brazilian Society of Clinical Analyses (SBAC). For the hematological and biochemical analyses, the samples were analyzed using a Poch 100iV Sysmex system (Kobe, Japan) and J & J Vitros 250 clinical system (Johnson & Johnson, USA), respectively.

Phenotypic analysis. The lymph nodes (LNs), Peyer's patches (PPs), and spleen (SPL) were removed macroscopically, weighed, and homogenized in RPMI 1640 medium (Gibco) using a cell strainer (BD). Cells were counted using a hemocytometer chamber and maintained om RPMI 1640 plus 10% fetal bovine serum (FBS; Gibco), 100 U/ml of penicillin, and 100 μg/ml of streptomycin until use.

Cells obtained from PPs, SPL, and MLNs were washed twice with phosphate-buffered saline (PBS), blocked for 45 min with 10% horse serum, washed again, and incubated for 1 h with fluorescein isothiocyanate-conjugated antibody against Mac-1 (CD11b; eBioscience, USA) or CD3 (eBioscience, USA). The cells were washed twice in PBS, and at least 10,000 events were obtained for each sample using a FACScan flow cytometer (Becton, Dickinson, USA).

The flow cytometry data were analyzed using the WinMDI program (Multiple Document Interface Flow Cytometry Application, version 2.8; The Scripps Research Institute, La Jolla, CA, USA). The percentage of cells positive for each antigen was applied to the total number of cells in each sample from each mouse to estimate the absolute number of cells of each cell type. The region of living cells was determined using the parameters forward scatter versus side scatter.

Identification of bacteria in intestinal tissue. The samples stained with Giemsa (Merck) and marked with 300 μM DAPI (4′,6-diamidino-2-phenylindole; Sigma-Aldrich) were used for the identification of invasive bacteria. For the fluorescence experiment, the tissue sections were permeabilized with Triton X-100 (Sigma-Aldrich), washed in PBS, stained in 300 μM DAPI for 1 min, washed in PBS again, and mounted with 0.5% *N*-propyl gallate (Sigma-Aldrich). Ten histological sections from five animals in each group were analyzed using light microscopy in the bright-field and epifluorescence (358- and 461-nm excitation and emission, respectively) modes. The images were obtained using a Nikon Eclipse 80i microscope equipped with a Nikon DS-Ri1 digital camera.

For fluorescence *in situ* hybridization (FISH), the cecum fragments were collected and fixed in 10% buffered formalin for 48 h. Subsequently, this tissue was incubated at 4°C in 10% and 30% sucrose for 24 h, posteriorly included in OCT gel (Tissue-Tek), and frozen in liquid nitrogen. Thin sections (5 μm) were recovered on slides prepared with polylysine (Sigma/Aldrich) on a cryostat (Leica CM1850). FISH was performed on each slide using the conditions and buffers described previously (56), using 30% formamide in the hybridization buffer and probes for eubacteria. After this procedure, the slides were marked with DAPI at a concentration of 0.1 μg/ml for 10 min, and the slide was coated with *N*-propyl gallate (Sigma/Aldrich) and observed with a Zeiss microscope equipped with an AxioImager AxioCam RMC microscope (Zeiss, Germany).

Macrophage experiments. Peritoneal macrophages were obtained by lavage of the peritoneal cavity with 10 ml of Dulbecco's modified Eagle medium (DMEM; Gibco, USA). After isolation from the peritoneal cavity, the monocytes-macrophages pass through an adhesion process and need to be maintained in culture for at least 3 days for stabilization (57). The number of total viable cells of mice, infected with *T. muris* or not, was determined using trypan blue (Sigma-Aldrich) in a Neubauer chamber. The numbers of peritoneal macrophages and cells of the RAW 264.7 macrophage cell line were counted (2×10^5 cells/well), and the cells were cultured in DMEM supplemented with 10% FBS, 100 U/ml penicillin, 100 μg/ml of streptomycin, and 2 mM glutamine in 24-well plates.

The production of nitric oxide (NO) was measured by determination of the nitrite (NO^{2-}) concentration in the supernatant using the Griess colorimetric method (58). In brief, peritoneal macrophages from control or infected mice were stimulated with 1 μg/ml of LPS for 24 h, and the amount of NO^{2-} in the supernatants was measured. The RAW 264.7 cell line was treated with ES products (10 μg/ml) for 24 h and was stimulated with LPS (10 ng/ml) for an additional 24 h, and then the NO^{2-} concentration in the supernatants was measured. The absorbance at 550 nm was measured by spectrophotometry, and the values were quantified against a sodium nitrite standard curve. After the experiment, to avoid any

variation in cell number, the cells in each well were lysed (the lysis buffer consisted of 0.1% Triton X-100 and a cOmplete protease inhibitor cocktail set [Sigma-Aldrich]), and the protein concentration was measured by the Bradford assay, based on the use of Coomassie brilliant blue G-250, using albumin as a standard (59). The nitrite concentration was related to the amount of proteins as the number of micromolar NO^{2-}/number of micrograms of protein.

Measurement of cytokine concentrations in immune organs, serum, and cell culture supernatants. Blood samples were obtained by cardiac puncture, allowed to clot at room temperature, and centrifuged at 500 × *g* for 10 min, and serum samples were collected and immediately frozen at −80°C until use. In addition, lymph nodes (LNs), PPs, SPL, and large intestine fragments were also collected and homogenized for cytokine analysis. Each 1 mg of LNs was homogenized in 100 μl PBS, and for large intestine fragments, we used the same weight (1 mg) with 50 μl PBS. The organs and tissues were immersed in ice-cold PBS supplemented with a complete protease inhibitor cocktail set (Sigma-Aldrich), washed, macerated, and passed through a 70-μm-mesh-size cell strainer (BD). After homogenization, the samples were centrifuged at 4°C and 500 × *g* for 15 min, and the supernatant was removed and immediately frozen at −80°C until use. The quantity of IL-1β in serum, LNs, and large intestine fragment supernatant was measured by use of an enzyme-linked immunosorbent assay (ELISA) kit, according to the manufacturer's instructions (Peprotech, USA). Cytokine (IL-2, IL-4, IL-6, IFN-γ, TNF-α, IL-17A, and IL-10) levels in serum, LNs, and large intestine fragment supernatant were determined using a commercial kit (cytometric bead array [CBA] mouse Th1/Th2/Th17; BD Pharmingen), according to the manufacturer's instructions. The supernatants were incubated with cytokine-specific antibody-coated microspheres and phycoerythrin (PE)-conjugated detection antibody at room temperature for 2 h with protection from the light. A standard curve was prepared by incubating the microspheres at different concentrations (0 to 5,000 pg/ml). After incubation, 500 μl of wash solution was added to each tube and the tubes were centrifuged at 200 × *g* for 5 min. The supernatant was discarded, and the pellet was resuspended in 300 μl of wash solution. Data were acquired on a FACSCanto II flow cytometer (BD Bioscience, USA) and analyzed using FCAP Array software (BD Bioscience). The cytokine detection limits were as follows: IL-2, 0.1 pg/ml; IL-4, 0.03 pg/ml; IL-6, 1.4 pg/ml; IFN-γ, 0.5 pg/ml; TNF-α, 0.9 pg/ml; IL-17A, 0.8 pg/ml; and IL-10, 16.8 pg/ml. The effects of ES products on IL-1β production were measured using RAW 264.7 macrophages incubated or not with ES products (10 μg/ml) for 24 h and then treated with 100 ng/ml LPS for 6 h. After this period, ATP (3 mM) was added and the mixture was incubated under the same conditions described above for an additional 2 h. The supernatants were collected, and the quantities of IL-1β and TNF-α were measured by use of an ELISA kit, according to the manufacturer's instructions, with a limit of detection of 10 pg/ml (Peprotech, USA).

Cell viability assays. Cell viability was assessed by the 3-(4,5-dimethylthiazol-2-yl)-2,5-diphenyltetrazolium bromide (MTT; Sigma-Aldrich) assay. RAW 264.7 macrophages (2×10^6 cells/ml) were allowed to adhere to 96-well tissue culture plates for 24 h at 37°C in an atmosphere of 5% CO_2. Macrophages were incubated with *T. muris* ES products (10 μg/ml) in the culture medium for 24 and 48 h. MTT (2.5 mg/ml) was added to the culture medium, and the culture was incubated for 3 h at 37°C. The resulting formazan crystals were solubilized by adding 10% dimethyl sulfoxide (DMSO) after removal of the supernatants. The absorbance of the culture at 570 nm was read using a microplate reader (Bio-Tek, Winooski, VT, USA). Untreated macrophages were lysed by the addition of 0.1% Triton X-100 as a positive toxicity control, and macrophages without any treatment were considered 100% viable.

Fecal cultures. To analyze the effects of the *T. muris* infection on the gut microbiota, about 0.09 g of feces, equivalent to approximately four fecal pellets, was collected immediately before the necropsy of five control mice and five infected mice. The fecal samples were maintained separately for each host. The animal stool was used for the cultivation of aerobic and anaerobic bacteria. For identification by biochemical tests, fresh stool samples from each animal were placed in tubes and diluted with 3 ml of PBS (for investigation of Gram-negative bacilli and enterococci) or 3 ml of thioglycolate broth (for investigation of total anaerobes and *Bacteroides* spp.). The samples were agitated on a mechanical shaker, and serial 10-fold dilutions were prepared in PBS or thioglycolate broth. Ten microliters of each dilution was plated in triplicate on the surface of the culture medium. For cultivation of the bacteria, Enterococcosel agar, blood agar, MacConkey agar, and brucella agar (all from Difco, USA) and bacteroides bile-esculin agar (Oxoid, UK) were used. The culture media were incubated at 37°C either under aerobic conditions or under anaerobic conditions using an anaerobic gas-generating kit in an anaerobic jar (Oxoid, UK) for 24 to 48 h. Following incubation, the number of CFU per 1 ml of fecal samples was calculated from the number of CFU per milliliter of the appropriate dilution obtained. Bacterial identification was carried out by biochemical tests. The identification of *Enterobacteriaceae* from the colonies grown on the MacConkey medium was performed by biochemical tests. The strains were seeded in the following media: double sugar-urea medium (DAU), sulfate-indole-agar motility medium (SIM; Kasvi) plus filter paper tape containing the Kovac reagent, and Simmons citrate medium (Kasvi). After sowing, the media were incubated in an oven at 37°C, and after 24 h, the result was read according to the variation in the color of the medium and turbidity indicating mobility or not.

The bacterial colonies identified by the biochemical tests, as explained above, were isolated on Trypticase soy agar (Oxoid, UK) for analyses using matrix assisted laser desorption ionization–time of flight (MALDI-TOF) mass spectrometry equipment (Microflex LT; Bruker). For bacterial species identification, MALDI Biotyper (version 3.1) software and FlexControl (version 3.4) software were used.

Statistical analyses. Differences among experimental groups in all the experiments were evaluated by the nonparametric Mann-Whitney test, with a P value of ≤ 0.05 being considered significant. All data were analyzed using GraphPad Prism (version 5) software and GraphPad InStat software (GraphPad, USA).

ACKNOWLEDGMENTS

We are grateful to the staff of the Fiocruz RPT12C platform and the Laboratory of Lipids platform (UERJ; LabLip platform) for hematological and biochemical analyses, Francisco Bolas-Fernandez from the Universidad Complutense de Madrid for the donation of *Trichuris muris* eggs, Pedro Ernesto Lopes Leão of the Microbiology Microscopy Center, Padrón-Lins-UFRJ, for support with the FISH experiments, and Sergio Fracalanzza and Larissa Alvarenga Batista Botelho from LIMM-UFRJ for mass spectrometry analyses. We thank Arian Carvalho de Alcantara for creation of the illustrations.

This work was supported by individual grants from the Brazilian agencies FAPERJ-JCNE (Productive Fellowship Program, grant 202.660/2018), CNPq, and CAPES for a Ph.D. scholarship and postdoctoral fellowship support.

REFERENCES

1. Global Burden of Disease Study 2013 Collaborators, World Health Organization. 2015. Investing to overcome the global impact of neglected tropical diseases. Third WHO report on neglected tropical diseases. World Health Organization, Geneva, Switzerland.
2. Global Burden of Disease Study 2013 Collaborators. 2015. Global, regional, and national incidence, prevalence, and years lived with disability for 301 acute and chronic diseases and injuries in 188 countries, 1990-2013: a systematic analysis for the Global Burden of Disease Study (2013). Lancet 386:743–800. https://doi.org/10.1016/S0140-6736(15)60692-4.
3. Amare B, Ali J, Moges B, Yismaw G, Belyhun Y, Gebretsadik S, Woldeyohannes D, Tafess K, Abate E, Endris M, Tegabu D, Mulu A, Ota F, Fantahun B, Kassu A. 2013. Nutritional status, intestinal parasite infection and allergy among school children in northwest Ethiopia. BMC Pediatr 13:7. https://doi.org/10.1186/1471-2431-13-7.
4. Reilly L, Nausch N, Midzi N, Mduluza T, Mutapi F. 2012. Association between micronutrients (vitamin A, D, iron) and schistosome-specific cytokine responses in Zimbabweans exposed to *Schistosoma haematobium*. J Parasitol Res 2012:128628. https://doi.org/10.1155/2012/128628.
5. Cafrune MM, Aguirre DH, Rickard LG. 1999. Recovery of *Trichuris tenuis* Chandler, 1930, from camelids (*Lama glama* and *Vicugna vicugna*) in Argentina. J Parasitol 85:961–962. https://doi.org/10.2307/3285836.
6. Tilney LG, Connelly PS, Guild GM, Vranich KA, Artis D. 2005. Adaptation of a nematode parasite to living within the mammalian epithelium. J Exp Zool A Comp Exp Biol 303:927–945. https://doi.org/10.1002/jez.a.214.
7. Briggs N, Weatherhead J, Sastry KJ, Hotez PJ. 2016. The hygiene hypothesis and its inconvenient truths about helminth infections. PLoS Negl Trop Dis 10:e0004944. https://doi.org/10.1371/journal.pntd.0004944.
8. Patel N, Kreider T, Urban JF, Jr, Gause WC. 2009. Characterisation of effector mechanisms at the host: parasite interface during the immune response to tissue-dwelling intestinal nematode parasites. Int J Parasitol 39:13–21. https://doi.org/10.1016/j.ijpara.2008.08.003.
9. Li RW, Wu S, Li W, Navarro K, Couch RD, Hill D, Urban JF, Jr. 2012. Alterations in the Porcine colon microbiota induced by the gastrointestinal nematode *Trichuris suis*. Infect Immun 80:2150–2157. https://doi.org/10.1128/IAI.00141-12.
10. Foth BJ, Tsai IJ, Reid AJ, Bancroft AJ, Nichol S, Tracey A, Holroyd N, Cotton JA, Stanley EJ, Zarowiecki M, Liu JZ, Huckvale T, Cooper PJ, Grencis RK, Berriman M. 2014. Whipworm genome and dual-species transcriptome analyses provide molecular insights into an intimate host-parasite interaction. Nat Genet 46:693–700. https://doi.org/10.1038/ng.3010.
11. Stroehlein AJ, Young ND, Korhonen PK, Chang BCH, Nejsum P, Pozio E, La Rosa G, Sternberg PW, Gasser RB. 2017. Whipworm kinomes reflect a unique biology and adaptation to the host animal. Int J Parasitol 7:857–866. https://doi.org/10.1016/j.ijpara.2017.04.005.
12. Klementowicz EJ, Travis AM, Grencis KR. 2012. *Trichuris muris*: a model of gastrointestinal parasite infection. Semin Immunopathol 34:815–828. https://doi.org/10.1007/s00281-012-0348-2.
13. Hurst RJM, Else KJ. 2013. *Trichuris muris* research revisited: a journey through time. Parasitology 140:1325–1339. https://doi.org/10.1017/S0031182013001054.
14. Lopes Torres EJ, De Souza W, Miranda K. 2013. Comparative analysis of *Trichuris muris* surface using conventional, low vacuum, environmental and field emission scanning electron microscopy. Vet Parasitol 196:409–416. https://doi.org/10.1016/j.vetpar.2013.02.026.
15. Hansen TVA, Hansen M, Nejsum P, Mejer H, Denwood M, Thamsborg SM. 2016. Glucose absorption by the bacillary band of *Trichuris muris*. PLoS Negl Trop Dis 10:e0004971. https://doi.org/10.1371/journal.pntd.0004971.
16. Harnett W. 2014. Secretory products of helminth parasites as immunomodulators. Mol Biochem Parasitol 195:130–136. https://doi.org/10.1016/j.molbiopara.2014.03.007.
17. Tritten L, Tam M, Vargas M, Jardim A, Stevenson MM, Keiser J, Geary TG. 2017. Excretory/secretory products from the gastrointestinal nematode *Trichuris muris*. Exp Parasitol 178:30–36. https://doi.org/10.1016/j.exppara.2017.05.003.
18. Briggs N, Wei J, Versteeg L, Zhan B, Keegan B, Damania A, Pollet J, Hayes KS, Beaumier C, Seid CA, Leong J, Grencis RK, Bottazzi ME, Sastry KJ, Hotez PJ. 2018. *Trichuris muris* whey acidic protein induces type 2 protective immunity against whipworm. PLoS Pathog 14:e1007273. https://doi.org/10.1371/journal.ppat.1007273.
19. Holm JB, Sorobetea D, Kiilerich P, Ramayo-Caldas Y, Estellé J, Ma T, Madsen L, Kristiansen K, Svensson-Frej M. 2015. Chronic *Trichuris muris* infection decreases diversity of the intestinal microbiota and concomitantly increases the abundance of lactobacilli. PLoS One 10:e0125495. https://doi.org/10.1371/journal.pone.0125495.
20. Houlden A, Hayes KS, Bancroft AJ, Worthington JJ, Wang P, Grencis RK, Roberts IS. 2015. Chronic *Trichuris muris* infection in C57BL/6 mice causes significant changes in host microbiota and metabolome: effects reversed by pathogen clearance. PLoS One 10:e0125945. https://doi.org/10.1371/journal.pone.0125945.
21. Hayes KS, Bancroft AJ, Goldrick M, Portsmouth C, Roberts IS, Grencis RK. 2010. Exploitation of the intestinal microflora by the parasitic nematode *Trichuris muris*. Science 328:1391–1394. https://doi.org/10.1126/science.1187703.
22. Wu S, Li RW, Li W, Beshah E, Dawson HD, Urban JF, Jr. 2012. Worm burden-dependent disruption of the porcine colon microbiota by *Trichuris suis* infection. PLoS One 7:e35470. https://doi.org/10.1371/journal.pone.0035470.
23. Else KJ, Finkelman FD, Maliszewski CR, Grencis RK. 1994. Cytokine-mediated regulation of chronic intestinal helminth infection. J Exp Med 179:347–351. https://doi.org/10.1084/jem.179.1.347.
24. Little MC, Bell LV, Cliffe LJ, Else KJ. 2005. The characterization of intraepithelial lymphocytes, lamina propria leukocytes, and isolated lymphoid follicles in the large intestine of mice infected with the intestinal nematode parasite *Trichuris muris*. J Immunol 175:6713–6722. https://doi.org/10.4049/jimmunol.175.10.6713.
25. Zaph C, Cooper PJ, Harris NL. 2014. Mucosal immune responses following intestinal nematode infection. Parasite Immunol 36:439–452. https://doi.org/10.1111/pim.12090.
26. DeSchoolmeester ML, Little MC, Rollins BJ, Else KJ. 2003. Absence of CC chemokine ligand 2 results in an altered Th1/Th2 cytokine balance and failure to expel *Trichuris muris* infection. J Immunol 170:4693–4700. https://doi.org/10.4049/jimmunol.170.9.4693.
27. Artis D, Potten CS, Else KJ, Finkelman FD, Grencis RK. 1999. *Trichuris muris*: host intestinal epithelial cell hyperproliferation during chronic infection is regulated by interferon-gamma. Exp Parasitol 92:144–153. https://doi.org/10.1006/expr.1999.4407.
28. Chenery AL, Antignano F, Hughes MR, Burrows K, McNagny KM, Zaph C. 2016. Chronic *Trichuris muris* infection alters hematopoiesis and causes

IFN-γ-expressing T-cell accumulation in the mouse bone marrow. Eur J Immunol 46:2587–2596. https://doi.org/10.1002/eji.201646326.
29. Batte EG, McLamb RD, Muse KE, Tally SD, Vestal TJ. 1977. Pathophysiology of swine trichuriasis. Am J Vet Res 38:1075–1079.
30. Lopes Torres EJ, Nascimento AP, Menezes AO, Garcia J, dos Santos MA, Maldonado A, Miranda K, Lanfredi RM, de Souza W. 2011. A new species of *Trichuris* from Thrichomys apereoides (Rodentia: Echimyidae) in Brazil: morphological and histological studies. Vet Parasitol 176:226–235. https://doi.org/10.1016/j.vetpar.2010.10.053.
31. Cunningham-Rundles S, McNeeley DF, Moon AJ. 2005. Mechanisms of nutrient modulation of the immune response. J Allergy Clin Immunol 115:1119–1128. https://doi.org/10.1016/j.jaci.2005.04.036.
32. Hughes S, Kelly P. 2006. Interactions of malnutrition and immune impairment, with specific reference to immunity against parasites. Parasite Immunol 28:577–588. https://doi.org/10.1111/j.1365-3024.2006.00897.x.
33. Katona P, Katona-Apte J. 2008. The interaction between nutrition and infection. Clin Infect Dis 46:1582–1588. https://doi.org/10.1086/587658.
34. Lee TDG, Wakelin D. 1983. Cortisone-induced immunotolerance to nematode infection in CBA/Ca mice. II. A model for human chronic trichuriasis. Immunology 48:571–577.
35. McKenzie GJ, Bancroft A, Grencis RK, McKenzie AN. 1998. A distinct role for interleukin-13 in Th2-cell-mediated immune responses. Curr Biol 8:339–342. https://doi.org/10.1016/s0960-9822(98)70134-4.
36. Ramanan D, Bowcutt R, Lee SC, Tang MS, Kurtz ZD, Ding Y, Honda K, Gause WC, Blaser MJ, Bonneau RA, Lim YAL, Loke P, Cadwell K. 2016. Helminth infection promotes colonization resistance via type 2 immunity. Science 352:608–165. https://doi.org/10.1126/science.aaf3229.
37. Ojha SC, Jaide C, Jinawath N, Rotjanapan P, Baral P. 2014. Geohelminths: public health significance. J Infect Dev Ctries 8:5–16. https://doi.org/10.3855/jidc.3183.
38. Pires AL, da Silveira TR, da Silva VD. 2003. Digital morphometric and stereologic analysis of small intestinal mucosa in well-nourished and malnourished children with persistent diarrhea. J Pediatr (Rio J) 79:329–336. https://doi.org/10.2223/JPED.1050.
39. Ok KS, Kim YS, Song JH, Lee JH, Ryu SH, Lee JH, Moon JS, Whang DH, Lee HK. 2009. *Trichuris trichiura* infection diagnosed by colonoscopy: case reports and review of literature. Korean J Parasitol 47:275–280. https://doi.org/10.3347/kjp.2009.47.3.275.
40. Khuroo MS, Khuroo MS, Khuroo NS. 2010. Trichuris dysentery syndrome: a common cause of chronic iron deficiency anemia in adults in an endemic area (with videos). Gastrointest Endosc 71:200–204. https://doi.org/10.1016/j.gie.2009.08.002.
41. Osazuwa F, Ayo OM, Imade P. 2011. A significant association between intestinal helminth infection and anaemia burden in children in rural communities of Edo State, Nigeria. N Am J Med Sci 3:30–44. https://doi.org/10.4297/najms.2011.330.
42. McSorley HJ, Maizels RM. 2012. Helminth infections and host immune regulation. Clin Microbiol Rev 25:585–608. https://doi.org/10.1128/CMR.05040-11.
43. Valero MA, Perez-Crespo I, Chillón Marinas C, Khoubbane M, Quesada C, Reguera- Gomez M, Mas-Coma S, Fresno M, Gironès N. 2017. *Fasciola hepatica* reinfection potentiates a mixed Th1/Th2/Th17/Treg response and correlates with the clinical phenotypes of anemia. PLoS One 12:e0173456. https://doi.org/10.1371/journal.pone.0173456.
44. Cortes I, Molinari JL, Solano S, Hernandez-Mendoza L, Ramirez A, Tato P. 2003. *Taenia solium* metacestode antigens which are protective for pigs induce Th1/Th2 mixed responses in mice. Parasitol Res 90:273–279. https://doi.org/10.1007/s00436-003-0855-0.
45. Myhill LJ, Stolzenbach S, Hansen TVA, Skovgaard K, Stensvold CR, Andersen LO, Nejsum P, Mejer H, Thamsborg SM, Williams AR. 2018. Mucosal barrier and Th2 immune responses are enhanced by dietary inulin in pigs infected with *Trichuris suis*. Front Immunol 9:2557. https://doi.org/10.3389/fimmu.2018.02557.
46. Eichenberger RM, Talukder MH, Field MA, Wangchuk P, Giacomin P, Loukas A, Sotillo J. 2018. Characterization of *Trichuris muris* secreted proteins and extracellular vesicles provides new insights into host-parasite communication. J Extracell Vesicles 7:1428004. https://doi.org/10.1080/20013078.2018.1428004.
47. D'Elia R, Else KJ. 2009. In vitro antigen presenting cell-derived IL-10 and IL-6 correlate with *Trichuris muris* isolate-specific survival. Parasite Immunol 31:123–131. https://doi.org/10.1111/j.1365-3024.2008.01088.x.
48. Leung JM, Budischak SA, Chung The H, Hansen C, Bowcutt R, Neill R, Shellman M, Loke P, Graham AL. 2018. Rapid environmental effects on gut nematode susceptibility in rewilded mice. PLoS Biol 16:e2004108. https://doi.org/10.1371/journal.pbio.2004108.
49. Cooper P, Walker AW, Reyes J, Chico M, Salter SJ, Vaca M, Parkhill J. 2013. Patent human infections with the whipworm, *Trichuris trichiura*, are not associated with alterations in the faecal microbiota. PLoS One 8:e76573. https://doi.org/10.1371/journal.pone.0076573.
50. Lee SC, Tang MS, Lim YA, Choy SH, Kurtz ZD, Cox LM, Gundra UM, Cho I, Bonneau R, Blaser MJ, Chua KH, Loke P. 2014. Helminth colonization is associated with increased diversity of the gut microbiota. PLoS Negl Trop Dis 8:e2880. https://doi.org/10.1371/journal.pntd.0002880.
51. Mansfield LS, Urban JF. 1996. The pathogenesis of necrotic proliferative colitis in swine is linked to whipworm induced suppression of mucosal immunity to resident bacteria. Vet Immunol Immunopathol 50:1–17. https://doi.org/10.1016/0165-2427(95)05482-0.
52. Jackson JA, Friberg IM, Little S, Bradley JE. 2009. Review series on helminths, immune modulation and the hygiene hypothesis: immunity against helminths and immunological phenomena in modern human populations: coevolutionary legacies? Immunology 126:18–27. https://doi.org/10.1111/j.1365-2567.2008.03010.x.
53. National Research Council. 2011. Guide for the care and use of laboratory animals, 8th ed. National Academies Press, Washington, DC.
54. National Health and Medical Research Council. 2013. Australian code for the care and use of animals for scientific purposes, 8th edition. Australian Government, Canberra, Australia.
55. Burkholder T, Foltz C, Karlsson E, Linton CG, Smith JM. 2012. Health evaluation of experimental laboratory mice. Curr Protoc Mouse Biol 2:45–165. https://doi.org/10.1002/9780470942390.mo110217.
56. Pernthaler J, Glöckner F-O, Schönhuber W, Amann R. 2001. Fluorescence in situ hybridization with rRNA-targeted oligonucleotide probes. Methods Microbiol 30:207–210. https://doi.org/10.1016/S0580-9517(01)30046-6.
57. Pimenta-Dos-Reis G, Torres EJL, Quintana PG, Vidal LO, Dos Santos BAF, Lin CS, Heise N, Persechini PM, Schachter J. 2017. POM-1 inhibits P2 receptors and exhibits anti-inflammatory effects in macrophages. Purinergic Signal 13:611–627. https://doi.org/10.1007/s11302-017-9588-x.
58. Granger DL, Taintor RR, Boockvar KS, Hibbs JB, Jr. 1996. Measurement of nitrate and nitrite in biological samples using nitrate reductase and Griess reaction. Methods Enzymol 268:142–151. https://doi.org/10.1006/meth.1995.1011.
59. Bradford MM. 1976. A rapid and sensitive method for the quantitation of microgram quantities of protein utilizing the principle of protein-dye binding. Anal Biochem 72:248–254. https://doi.org/10.1016/0003-2697(76)90527-3.